

# The Femto-experiment for the LHC: The $W$ -boson beams and their targets<sup>\*</sup>

M. W. Krasny<sup>a</sup>, S. Jadach<sup>b</sup> and W. Płaczek<sup>c</sup>

<sup>a</sup>*LPNHE, Pierre and Marie Curie University, Tour 33, RdC,  
4, pl. Jussieu, 75005 Paris, France,*

<sup>b</sup>*Institute of Nuclear Physics Polish Academy of Sciences,  
ul. Radzikowskiego 152, 31-342 Cracow, Poland,*

<sup>c</sup>*Marian Smoluchowski Institute of Physics, Jagiellonian University,  
ul. Reymonta 4, 30-059 Cracow, Poland.*

## Abstract

The LHC has been designed as a collider of proton and ion beams. However, in its experimental program, which is focused mainly on studies of high energy transfer collisions of Standard Model point-like particles, protons and ions will play a backstage role. For the majority of the LHC experimentalists, their role will be confined to providing standardized, acceleration-process-stable envelopes for tunable-density and tunable-isospin bunches of Standard Model constituents: quarks and gluons. The inter-bunch environment of collisions of these Standard Model particles specific to hadronic colliders and absent in the leptonic ones, has always been considered as a burden – an annoying but unavoidable price to pay for increasing the collision-energy of point-like particles in the storage rings. In this paper we shall argue that such a burden can be converted into an important merit of the high-energy hadronic colliders – a corner-stone for a fermi-length-scale “collision-experiment” employing the bunches of spectator quarks and gluons as tunable “femtoscopic” targets for the beams of short-living electroweak bosons.

*To be submitted to Physical Review D*

**TPJU-3/2005  
March 2005**

---

<sup>\*</sup>The work is partly supported by the program of cooperation between the IN2P3 and Polish Laboratories No. 05-116, and by the EC FP5 Centre of Excellence “COPIRA” under the contract No. IST-2001-37259.

# 1 Introduction

Perhaps the most important remaining open-question for the quantum-field-theory-based description of interactions of the basic building blocks of matter is the mechanism which drives the high-energy interactions of longitudinally and transversely polarized, massive electroweak bosons. The Higgs model and its known extensions provide a set of possible scenarios for such a mechanism. These scenarios are very attractive because they provide an abundant supply of road-maps and the corresponding navigation rules which could be simply picked-up and followed while exploring, at the LHC collider, the “*Terra incognita*” of the TeV-energy-scale interactions of electroweak bosons. By applying these rules the exploration process is reduced to the painstaking scenario-scrutinizing process. Such a strategy has two important merits: it is theoretically well-controlled and experimentally well-defined. But it has also a price to pay: it involves a considerable risk of overlooking new, unexpected phenomena.

To minimize such a risk, we would like to advocate a complementary strategy focusing on the development of handy experimental tools for the exploration process in parallel to mastering the discovery-guide recipes. Obviously, the most desirable tool for exploring the high-energy interactions of the electroweak bosons would be a luminous, polarized, high-energy beam of electroweak bosons. If proton beams of energies exceeding  $10^{17}$  GeV were available, secondary beams of electroweak bosons could be easily formed and used in dedicated experiments – in close analogy to fixed target muon-beam experiments which routinely use beams of unstable particles.

The central point of the present and of the forthcoming paper [1] is that, even if experiments using beams of electroweak bosons cannot be realized at the macroscopic length-scales, the LHC collider offers a reduced-scope, yet unique opportunity to realize them at the femtosopic length-scale.

The luminous, high-energy LHC collider will be a very efficient factory to copiously produce the electroweak bosons. Its unique merit, with respect to other machines, is that these short-living particles could be observed at the LHC collider over sufficiently long time for experimental “femtoscopic” studies of their properties and interactions. The electroweak bosons will travel, for the observers co-moving with the LHC bunches, over the atomic distances of up to  $10^4$  fm before decaying. This defines the maximal lengths, thus the type, of possible targets which, if arranged to co-move with the LHC bunches, could be employed in experimental studies of properties and collisions of the electroweak bosons. Nature provides only one type of target satisfying the above criteria – the atomic nucleus.

Nuclear beams will play a double role in the proposed scheme. First of all, they will provide standardized bunches of quarks and gluons of the adjustable isospin, allowing to tune the fluxes of the electroweak bosons. In addition, they will supply the co-moving, hadronic matter of adjustable length, which will serve in forming the

effective targets for the beam of electroweak bosons.

The terms *beam of electroweak bosons* and *effective target* are precisely defined in Sections 3 and 4 of this paper. They will be used here in direct analogy to the beam and targets being used in the muon scattering experiments. The creation of the beam of electroweak bosons in collisions of fixed-isospin partonic-bunches is considered here to be equivalent to the processes of creation of the muon beam from the fixed-flux and flavour-composition beams of secondary hadrons. Hard partonic collisions creating the electroweak boson beam are uncorrelated with the subsequent collisions of the produced  $W$ -boson beam particles with bunches of spectator quarks and gluons because of the large Lorentz- $\gamma$  factor of the colliding partonic bunches, high mass of electroweak bosons, and their colourless nature. This factorization is analogous to the factorization of the production and collisions of the muon beam. The length of the target for the electroweak boson beam, contrary to the fixed-length target for the muon beam, will vary on event-by-event basis depending upon the localization of the space-time volume, within the bunch of quarks and gluons, where the beam particle was created. The average length of the target, however, will be fixed for the fixed atomic number of the primary beam particles. This quantity defines the *effective-target* length.

The most important difference between using the muon beam in a concrete experiment and using the electroweak boson beam is that the former one can be isolated by the suitable absorber and the beam transport system while the latter one cannot be fully isolated from the beams of spectator quarks and gluons, and from the produced hadrons. Therefore, special measurement procedures and unfolding methods must be invented to filter out, as much as possible, the electroweak boson collision signals from the noise of ordinary collisions of quarks and gluons.

The discussion of such procedures and methods will be presented in a dedicated paper and is not discussed here. This paper is devoted to the beam aspects of the femtoscopic experiment. We shall pick-up the the beam of charged electroweak bosons, namely  $W^+$  and  $W^-$ , and present its properties, methods of controlling its intensity, momentum-band, polarization and the luminosity of the  $W$ -nucleon collisions.

## 2 Gedanken experiment

If Planck-energy-scale antineutrino beams were available, then configuring a fixed target experiment to study the properties and the collisions of polarized  $W$ -bosons could follow directly the examples of the CERN fixed target experiments which use the polarized muon beams. Polarized  $W$ -bosons produced in collisions of the antineutrinos with a polarized low-energy electron beam would travel the distance larger than 1 kilometer before decaying. Thus, there would be a sufficient space for:

(1) filtering out the annihilation processes, (2) selecting a narrow momentum band of the produced  $W$ -beam, (3) measuring the  $W$ -boson macroscopic electric current, (4) placing a suitable collision target, (5) identifying and measuring the products of the  $W$ -boson collisions. For example, the inclusive cross section,  $\sigma_{incl}^{\lambda_{in}}$ , for scattering of polarized  $W$ -bosons on nucleons could be derived from the measurements by using the canonical formula:

$$N_{incl}^{\lambda_{in}}(s_{Wn}, p_W^{out}) = \mathcal{F}_W^{\lambda_{in}}(s_{Wn}) \sigma_{incl}^{\lambda_{in}}(s_{Wn}, p_W^{out}) \rho_t l_t , \quad (1)$$

where  $N_{incl}^{\lambda_{in}}(s_{Wn}, p_W^{out})$  is the observed rate of events at the  $W$ -nucleon centre-of-mass-system (CMS) energy squared  $s_{Wn}$ , in which the momentum of the outgoing  $W$ -boson is  $p_W^{out}$ .  $\mathcal{F}_W^{\lambda_{in}}(s_{Wn})$  is the flux of  $W$ -bosons having the polarization  $\lambda_{in}$ ,  $\rho_t$  is the target density, and  $l_t$  is the target length.

Applying this formula to the Planck-energy experimental configuration requires two conditions, always taken for granted in the fixed target muon experiments, to be fulfilled:

- The  $W$ -boson beam must be formed before arriving at the position of the target.
- The total distance between the beam creation zone and the exit point of the target must be significantly smaller than  $c\tau = \gamma_W c\tau_W$ , where  $\gamma_W$  is the  $W$ -boson beam Lorentz factor,  $\tau_W$  is the lifetime of the  $W$ -boson in its rest frame and  $c$  is the speed of light in the vacuum.

In our ‘gedanken experiment’ they are fulfilled owing to the selection of the point-like annihilation process as the source of the  $W$ -boson beam and owing to the Planck-scale  $\gamma_W$  factor which, in the rest frame of the target, assures macroscopic distances over which the  $W$ -boson could travel before its disintegration.

Such an experiment cannot be presently realized. However, as we shall show in the following section, a reduced scope of its functions can be realized at the femtosopic scale using the LHC beams. The LHC beams, that will be employed in configuring such an experiment are the proton and the deuteron beams colliding with the heavy ion beams. The collisions of these beams will be referred to, in the following, as the nucleon–nucleus collisions.

## 3 The femto-experiment

### 3.1 Femto-picture

Given the ratio of the LHC beam energy to the Planck-scale energy, the LHC experiment to study the  $W$ -boson properties and its collisions must be configured at the

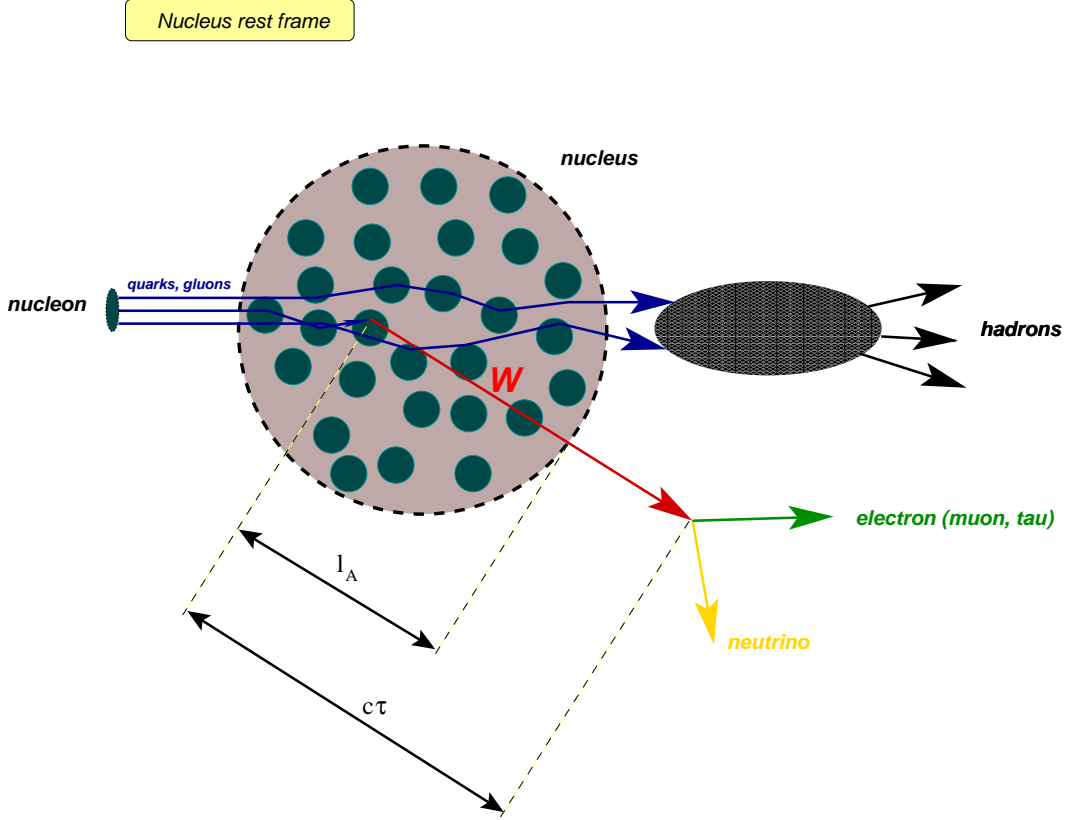


Figure 1: The factorization of the  $W$ -production and  $W$ -collision processes.

fermi-length scale. It is thus bound to use the nuclear medium to form the beam of  $W$ -bosons and to observe their interactions. The nucleus will be considered, in the processes discussed in this paper, as a classical object described fully by its static parameters. Its dynamic quantum degrees of freedom can be safely neglected in the following discussion.

The nucleus-rest-frame space-time picture of production of a  $W$ -boson in nucleon-nucleus collisions, its passage in the hadronic matter and subsequent decay is shown in Fig. 1. In the nucleus rest frame, the incoming nucleon can be considered, for the Lorentz factor  $\gamma \gg 1$ , as a Lorentz-frozen (static) bunch of independent partons (quarks and gluons). The  $W$ -boson is produced in the hard collision of one its partons with the target nucleus. The produced  $W$ -boson travels the distance  $l_A$  in the nucleus, then leaves the nucleus, and decays at the distance  $c\tau = c\tau_W\gamma_W$ .

Three requirements must be satisfied to “configure” the nucleon–nucleus collisions at the LHC as a femtoscopic experiment to explore the high-energy interactions of the  $W$ -bosons with hadronic matter. The necessity to fulfill these requirements

determines which of the functions of the ‘gedanken experiment’ can be realized at the LHC. They are discussed below in turn.

## 3.2 Event selection

The first requirement is to define the experimental signatures, and to provide the effective selection methods for those of the nucleon–nucleus collisions which contain the signals of the  $W$ -collisions with hadronic matter. Contrary to the ‘gedanken experiment’ the  $W$ -boson collision events cannot be directly selected. As a consequence the scope of exploring the  $W$ -collision processes must be limited to the inclusive  $W$ -nucleon collisions,  $W + \text{nucleon} \rightarrow W + X$ . The  $W$ -boson collision effects, and the effects of the absorption of the  $W$ -bosons in hadronic matter will be studied using the sample of events characterized by the final-state  $W$ -boson signatures. These effects will have to be filtered out from the effects due to the initial state interaction of the partons producing the  $W$ -bosons, and from the overwhelming “noise” of simultaneous collisions of co-moving beams of strongly interacting partons. The filtering methods will be proposed and their sensitivity to the  $W$ -collision effects will be discussed in [1].

## 3.3 Framework

### 3.3.1 Factorization

The second requirement is to provide a framework, similar to that for the ‘gedanken experiment’, which will allow to express the nucleon–nucleus collision observables exclusively in terms of the  $W$ -nucleon inclusive cross section and experimentally controllable quantities. For simplicity we consider first the framework for the inclusive scattering of unpolarized  $W$ -bosons,  $W + \text{nucleon} \rightarrow W + X$ . This framework will be extended in Section 3.3.5 by including the polarization effects, and in Section 3.6 by including the  $W$ -boson absorption effects.

The framework is based upon a decomposition of the process shown in Fig. 1 into the three **independent** processes of: the creation of the  $W$ -boson, its propagation in hadronic matter, and its decay. We propose the following factorized form of the Born-level matrix element for the process shown in Fig. 1:

$$\begin{aligned} \mathcal{M}(p_n, p_A, p_W^{in}, r, p_W^{out}, p_1, p_W^{out} - p_1 | A) = \\ \mathcal{M}_f(p_n, p_A, p_W^{in}, r | A) \mathcal{M}_p(p_W^{in}, p_W^{out}, l_A(p_W^{in}, p_A, r)) \mathcal{M}_d(p_1, p_W^{out} - p_1), \end{aligned} \quad (2)$$

where  $\mathcal{M}_f(p_n, p_A, p_W^{in}, r | A)$  is the amplitude for the  $W$ -boson formation in the collision of the nucleon, carrying the momentum  $p_n$ , with the nucleus of the atomic number  $A$ , carrying the momentum  $p_A$ . The  $W$ -boson is created at the position  $r$

and carries the momentum  $p_W^{in}$ . The amplitude  $\mathcal{M}_p(p_W^{in}, p_W^{out}, l_A(p_W^{in}, p_A, r))$  represents the propagation amplitude of the produced  $W$ -boson in hadronic matter over the distance  $l_A$  leading to a change of its momentum to  $p_W^{out}$ . This amplitude includes undisturbed propagation of the  $W$ -boson - in such a case  $p_W^{in} = p_W^{out}$ . The amplitude  $\mathcal{M}_d(p_1, p_W^{out} - p_1)$  is the decay amplitude of observing the  $SU(2)_L$ -doublet particles of the momenta  $p_1$  and  $p_W^{out} - p_1$  in the decay of the  $W$ -boson. In the above formulas the symbols representing kinematic and space variables are **three-vectors**.

Four properties of the above factorization scheme are important.

- The  $W$ -boson propagation amplitude,  $\mathcal{M}_p$ , does not depend upon the mechanism of the  $W$ -boson formation. It depends only upon its momentum.
- $\mathcal{M}_p$  depends upon the position of the  $W$ -boson creation point,  $r$ , only via the  $W$ -boson momentum dependent effective path-length of the  $W$ -boson in the hadronic matter,  $l_A$ .
- The decay amplitude,  $\mathcal{M}_d$ , is independent of the  $W$ -boson creation point and of the atomic number of the nucleus. It depends only upon the momentum of the  $W$ -boson exiting the hadronic matter which, in turn, is unambiguously determined by the momenta of its decay products.
- The momenta of the incoming and of the outgoing  $W$ -boson are described by three-vectors rather than by four-vectors.

Such a simple factorization does not work in general. It requires several conditions to be satisfied. The reasons why it works for  $W$ -bosons produced at the LHC collider are discussed below.

### 3.3.2 The case of $W$ -bosons at LHC

The factorization is a direct consequence of the following facts:

- The  $W$ -boson is a point-like particle.
- The  $W$ -boson is a colour-neutral particle<sup>1</sup>.
- The mass of the  $W$ -boson is substantially larger than any scale of the strong interactions.
- The LHC energy is sufficiently high for the  $W$ -boson decay length to be larger than the total distance between the  $W$ -boson creation point and the point where it exits the nuclear medium.

---

<sup>1</sup>While the former condition assures that the formation of the  $W$ -boson is an instantaneous process, the present one assures that a colour-neutral object is instantaneously produced. Note, that none of the above two conditions is fulfilled in production of the  $J/\Psi$  particle.

- The  $W$ -bosons arriving at the position of the target can be considered as free on-shell particles.

The first three of them are obvious. The last two are discussed below.

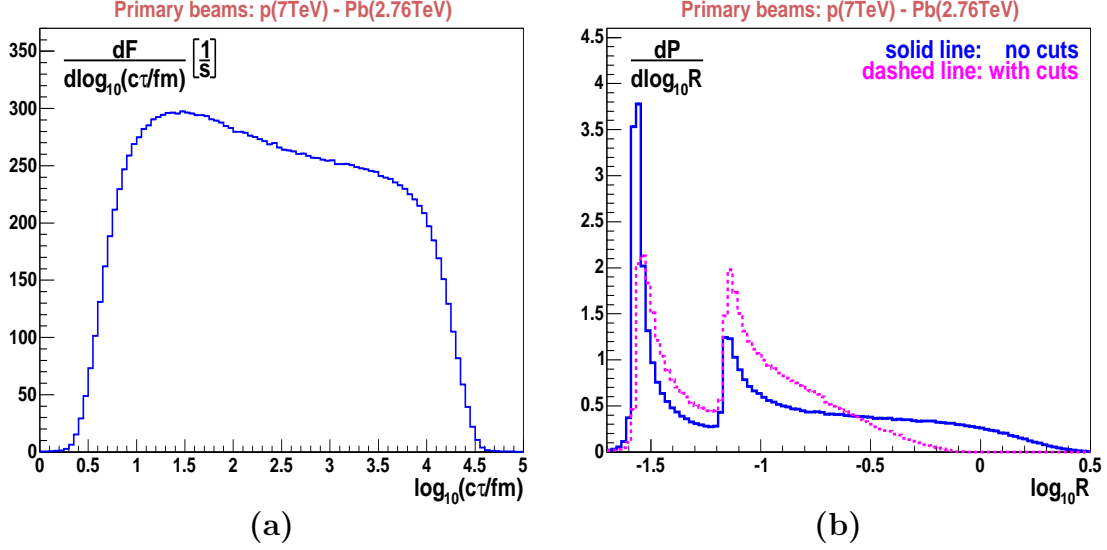


Figure 2: The distributions of: (a) the  $W$ -boson lifetime and (b)  $\log_{10} R$ . See the text for more details.

In Fig. 2a we show the distribution of the logarithm of the total path-length,  $c\tau$ , of  $W$ -bosons produced in the  $p$ - $Pb$  collisions, measured in the rest frame of the  $Pb$ -bunches<sup>2</sup>. Before decaying, the  $W$ -bosons formed in the collisions of the fastest (mainly valence) quarks of the incoming nucleon, travel the distance of  $\sim 10^4$  fm, while those formed in collisions of the slowest (mainly sea) quarks of the incoming nucleon travel the distance of  $\sim 10$  fm.

The  $W$ -bosons are produced in the process of Drell–Yan-like annihilation of quarks and antiquarks<sup>3</sup>. The quantum-uncertainty of the longitudinal position  $z$  of the quark–antiquark annihilation process with respect to the position of the nucleus is determined by the momentum of the quark (antiquark) which has been removed

<sup>2</sup>We postpone the discussion of Monte Carlo generator, which was used to produce this plot, till the next section.

<sup>3</sup>Formally, the partonic picture of hadrons is valid in the infinite-momentum frame, e.g. in the rest frame of the LHC experiments. In this frame the  $W$ -boson formation can be pictured as the annihilation of the  $SU(2)_L$ -partner partons. In the nucleus rest frame the same process can be pictured as the bremsstrahlung of the  $W$ -boson from the incoming nucleon’s quark. The results and conclusions presented in this paper do not depend upon the choice of the reference frame.



from the nucleus. In the rest frame of the nucleus it is uncertain within the Ioffe-length [2]:

$$L_{\text{Ioffe}}(x_A) = \frac{1}{2M_A x_A}, \quad (3)$$

where  $M_A$  is the mass of the nucleus and  $x_A = p_{\text{parton}}/p_{\text{nucleus}}$  is the infinite-momentum-frame fraction of the nucleus momentum carried by the parton taking part in formation of the  $W$ -boson. Note, that for those of partons which can be associated to the individual nucleons of the nucleus:  $x_A = p_{\text{parton}}/(A p_{\text{nucleon}}) = x_N/A$ , if the effects of the nucleon Fermi motion is neglected. The annihilation process can thus be localized, within the volume of the individual nucleons of the nucleus if  $x_A \sim M_N/M_A$ , or, at the LHC energies, up to the distances of  $L_{\text{Ioffe}} \sim 10^3$  fm, if the annihilation process involves the quark (antiquark) carrying the infinite-momentum-frame fraction  $x_A \sim 10^{-4} M_N/M_A$  of the nucleus momentum.

In order to show that the LHC energy is sufficiently high for the  $W$ -boson decay length to be larger than the total distance between the position  $r$  of the quark-antiquark annihilation and the position where the  $W$ -boson exits the nuclear medium we construct, for each annihilation event, the ratio  $R$  defined as:

$$R = \frac{\langle l_A \rangle + L_{\text{Ioffe}}}{c\tau_W \gamma_W}. \quad (4)$$

where  $\langle l_A \rangle$  is the average path-length of the  $W$ -boson in hadronic matter for the  $W$ -bosons created within the volume of the nucleus<sup>4</sup>. In order to satisfy the discussed requirements, this ratio must be  $< 1$ , both for the large momentum  $W$ -bosons, for which  $\langle l_A \rangle \ll L_{\text{Ioffe}}$ , and for the small momentum  $W$ -bosons, for which  $\langle l_A \rangle \gg L_{\text{Ioffe}}$ . In Fig. 2b we show the probability distribution of  $\log_{10} R$  for the  $W$ -bosons produced at the LHC in the collisions of protons with the lead nuclei. The solid line represents the full sample of  $W$ -bosons, while the dashed line the sample which satisfies the canonical LHC trigger requirements [3] for selection of the  $W$ -boson events. Both plots are normalized such that they represent the probability distributions. It is evident that the trigger acceptance cut removes the  $R \geq 1$  tail of the distributions which is populated by events in which the  $W$ -boson is produced by the valence quarks of the nucleus and the very slow antiquarks of the nucleon. At the LHC, all registered  $W$ -bosons have their decay length larger than the distance between their creation point and the point where they leave the hadronic matter<sup>5</sup>. It is worthwhile to note that, if one considers only the leading order process of the  $W$ -boson production, and if the  $W$ -boson momentum satisfies  $\langle l_A \rangle \ll L_{\text{Ioffe}}$ , then  $R = \Gamma_W/M_W$  for massless quarks, where  $M_W$  is the  $W$ -boson mass and  $\Gamma_W$  is its total decay width.

---

<sup>4</sup>The calculation of this quantity is presented in Section 5.

<sup>5</sup>The residual probability that the  $W$ -bosons produced in the nucleon-nucleus collisions decay inside the nucleus can be controlled **experimentally** by studying the photon radiation yield in events in which the  $W$ -boson decays into the electron and the neutrino.

In the leading process of the  $W$ -boson formation, the longitudinal size of the  $W$ -boson formation cell<sup>6</sup>,  $\delta z = \gamma_W/M_W$ , is equal to the quantum uncertainty of the position of the nucleus with respect to the  $W$ -boson creation point, irrespectively of the  $W$ -boson momentum. The nuclear-rest-frame picture of the process is the following one. The quark (antiquark) of the incoming nucleon emits a virtual  $W$ -boson. The quark(antiquark)–virtual- $W$ -boson pair travels until the quark (antiquark) is absorbed within the nucleus. Slow quarks are absorbed at the nucleus surface while the fast ones are absorbed within the volume of one of the nucleon of the nucleus. The  $W$ -boson becomes a free, on-shell particle as soon as its companion quark is absorbed. In subsequent collisions the  $W$ -bosons can be considered as free, on-shell particles<sup>7</sup>.

Two examples illustrating the space time picture of the  $W$ -formation and decay process at the LHC energies are given below. For  $W$ -bosons produced at the lowest trigger-accepted  $\gamma_W \sim 10^2$ , the nuclear-rest-frame size of their formation cell of the order of 0.25 fm. These  $W$ -bosons are produced mainly by the valence quarks of the nucleus, i.e. they are fully formed within the volume of a nucleon within a nucleus. For subsequent interactions with the spectator nucleons they are free on-shell particles. They travel the distance of  $\sim 10$  fm before decaying. For the  $W$ -bosons produced at the highest trigger-accepted  $\gamma_W = 10^5$  the nuclear-rest-frame size of the their formation cell is by two orders of magnitude greater than the nucleus size. These  $W$ -bosons are produced by the fastest quarks of the incoming nucleon by bremsstrahlung of the  $W$ -boson at the distance of  $\sim 10^3$  fm from the nucleus centre. They become fully formed on-shell particles at the nucleus surface where its companion quark (antiquark) is absorbed. Their decay length is  $\sim 10^4$  fm.

### 3.3.3 Amplitudes and probabilities

The  $W$ -boson propagation amplitude  $\mathcal{M}_p$  could, in principle, be modeled and implemented in dedicated Monte Carlo programs. One could then try to unfold its selected properties from the analysis of the measured observables of the nucleon-nucleus collisions. The goal of the femto-experiment is, however, to directly measure the  $W$ –nucleon collision observables. These observables must thus be expressed only

---

<sup>6</sup>The  $W$ -bosons are created quasi instantaneously. In the rest frame of the  $W$ -boson the size of the  $W$ -boson formation cell that satisfies the Heisenberg uncertainty principle is:  $\delta r \sim 1/M_W$ , where the  $W$ -boson mass  $M_W$  is expressed in the units in which  $c = 1$  and the Planck constant  $\hbar = 1$ .

<sup>7</sup>The **experimental** procedure to demonstrate that the  $W$ -bosons were formed before colliding in nuclear matter would be straightforward if the remnants of the nucleus and of the nucleon were measured. Such a procedure would then be equivalent to that used in the analysis of tagged photoproduction events at the HERA collider. At the LHC, the off-shellness of the  $W$ -bosons will be partially controlled by studying the topology of the particle flow in the analyzed sample of events with the final  $W$ -boson signature.

in terms of the squares of the amplitudes and must not depend upon the variables which cannot be measured. In order to show that such measurements are feasible, we have to integrate the matrix element  $\mathcal{M}$  over each of the variables that could never be determined experimentally (whatever experimental set-up is proposed), and to calculate its square.

In the process shown in Fig. 1 the momentum of the produced  $W$ -boson could in principle be determined by measuring the remnants of the nucleon and of the nucleus and by measuring the energy flow of the  $W$ -recoil jet<sup>8</sup>. The momentum of the outgoing  $W$ -boson could be determined by measuring the momenta of outgoing leptons (even if measuring the neutrino momentum would be highly unpractical).

The remaining integrals are thus those over the unobserved position of the  $W$ -boson creation point,  $(x, y, z)$ :

$$\begin{aligned} |\mathcal{M}_{int}|^2 &= \int dx \int dy \int dz |\mathcal{M}(x, y, z)|^2 \\ &= \int dx \int dy \int dz |\mathcal{M}_f(x, y, z) \mathcal{M}_p(l_A(x, y, z)) \mathcal{M}_d|^2, \end{aligned} \quad (5)$$

where we have left over, for simplicity, the dependence of the amplitudes upon the kinematic variables.

The above expression can be simplified. As we have discussed in the previous section, each of the  $W$ -bosons produced in the primary collision, irrespective of its momentum, is “fully formed” before arriving at the position of the target. In addition, as we shall discuss in detail in Section 5, its path-length in hadronic matter is independent of the exact formation-point position within the  $W$ -boson production cell. Therefore the  $(x, y, z)$ -dependence of the relative phases of the  $\mathcal{M}_f$  and  $\mathcal{M}_p$  amplitudes can be neglected and the position of the  $W$ -boson creation point can be replaced by the “coarser granularity” position of the  $W$ -boson formation cell:  $(x_p, y_p, z_p)$ . Consequently the formula (5) can be written in the following form:

$$|\mathcal{M}_{int}|^2 = |\mathcal{M}_d|^2 \int dx_p \int dy_p \int dz_p |\mathcal{M}_f(x_p, y_p, z_p)|^2 |\mathcal{M}_p(l_A(x_p, y_p, z_p))|^2. \quad (6)$$

We have, so far, demonstrated that the partonic collisions producing the  $W$ -bosons can be considered, in the studies of the  $W$ -boson propagation in the nuclear medium, as a probabilistic random emission source producing the  $W$ -boson beam. The only difference of such a beam with respect to the  $W$ -beam of the ‘gedanken

---

<sup>8</sup>The ambiguity of assigning a fraction of particles produced in the inelastic collisions of  $W$ -bosons to the remnants, and/or to the recoil jet could, in principle, lead to residual interference effects for  $W$ -bosons produced at very small transverse momenta. This effect is neglected in this paper. Note, that the  $W$ -boson recoil particles could, in principle, be fully resolved from the particles produced in the  $W$ -boson collisions owing to the lack of the colour interconnection between these two systems.

experiment' is that its source is randomly distributed in space within the nuclear volume and, for the high-momentum  $W$ -bosons, outside the nuclear volume.

### 3.3.4 Cross sections

The factorized form of the integral (6) allows us to directly link the rate of those of the nucleon–nucleus collision events shown in Fig. 1, in which the produced  $W$ -boson collided in the nucleus, to the the  $W$ -nucleon collision inclusive cross section. Indeed, the factorization of the squared amplitudes allows us to express the rate  $\mathcal{N}_{evt}$  in the following form:

$$\mathcal{N}_{evt}(p_n, p_A, p_W^{in}, p_W^{out}, p_1|A) = \int dx_p \int dy_p \int dz_p \mathcal{N}_W(p_n, p_A, p_W^{in}, x_p, y_p, z_p|A) \quad (7)$$

$$\times \sigma_{Wn}^{incl}(p_W^{in}, p_W^{out}) l_A(x_p, y_p, z_p, p_W^{in}, p_A) \rho_A(p_A) \mathcal{P}_{decay}(p_1, p_W^{out} - p_1)$$

where  $\mathcal{N}_W(p_n, p_A, p_W^{in}, x_p, y_p, z_p|A)$  is the unit volume-rate of the  $W$ -bosons produced at the cell-position  $(x_p, y_p, z_p)$ ,  $\sigma_{Wn}^{incl}(p_W^{in}, p_W^{out})$  is the  $W$ -nucleon collision inclusive cross section,  $l_A(x_p, y_p, z_p, p_W^{in}, p_A)$  is the path-length of the  $W$ -boson in the nucleus characterized by its atomic number  $A$  and the nuclear density<sup>9</sup>  $\rho_A(p_A)$ , and  $\mathcal{P}_{decay}(p_1, p_W^{out} - p_1)$  is the probability of the decay of the  $W$ -boson having the momentum  $p_W^{out}$  into the  $SU(2)_L$ -doublet leptons of the four-momenta  $p_1$  and  $p_W^{out} - p_1$ . The above formula is valid for the  $W$ -nucleon cross section  $\sigma_{Wn} \ll 1 \text{ fm}^2$ . This condition assures that the  $W$ -boson interacts at most once within the nuclear volume.

The result of the integration is:

$$\mathcal{N}_{evt}(p_n, p_A, p_W^{in}, p_W^{out}, p_1|A) = \mathcal{F}_W(p_n, p_A, p_W^{in}|A) \quad (8)$$

$$\times \sigma_{Wn}^{incl}(p_W^{in}, p_W^{out}) \langle l_A(p_W^{in}, p_A) \rangle \rho_A(p_A) \mathcal{P}_{decay}(p_1, p_W^{out} - p_1),$$

where  $\mathcal{F}_W(p_n, p_A, p_W^{in}|A)$  is the total flux of the  $W$ -bosons, and

$$\langle l_A(p_{in}^W, p_A) \rangle = \int dx_p \int dy_p \int dz_p \mathcal{P}_W(p_n, p_A, x_p, y_p, z_p, p_{in}^W|A) l_A(x_p, y_p, z_p, p_{in}^W, p_A) \quad (9)$$

is the average path-length of the  $W$ -boson in hadronic matter. In this formula  $\mathcal{P}_W$  is the probability density to produce the  $W$ -boson carrying the momentum  $p_{in}^W$  within the formation cell positioned at  $r_p = (x_p, y_p, z_p)$ . It is formally expressed as:

$$\mathcal{P}_W(p_n, p_A, x_p, y_p, z_p, p_{in}^W|A) = \frac{\mathcal{N}_W(p_n, p_A, x_p, y_p, z_p, p_{in}^W|A)}{\int dx_p \int dy_p \int dz_p \mathcal{N}_W(p_n, p_A, x_p, y_p, z_p, p_{in}^W|A)}. \quad (10)$$

<sup>9</sup>Note, that the path-lengths and the nuclear density must be calculated in the reference frame in which the kinematic variables are determined.

The formula (9) becomes particularly simple if explicitly integrated over the outgoing lepton momentum  $p_1$ . Since the integrated decay probability is equal to 1, the lepton-momentum integrated rate can be expressed as<sup>10</sup>:

$$\mathcal{N}_{evt}(p_n, p_A, p_{in}^W, p_{out}^W | A) = \mathcal{F}_W(p_n, p_A, p_{in}^W | A) \sigma_{Wn}^{incl}(p_{in}^W, p_{out}^W) \langle l_A(p_{in}^W, p_A) \rangle \rho_A(p_A). \quad (11)$$

The above formula, if written in the Lorentz-reference frame in which the nucleus is at rest and the  $W$ -boson has only the longitudinal component of its momentum:  $p_W^{in} = (0, 0, \sqrt{[s_{Wn} - (M_W + M_n)^2][s_{Wn} - (M_W - M_n)^2]}/2M_n, (s_{Wn} - M_W^2 - M_n^2)/2M_n)$ , where  $s_{Wn}$  is the CMS energy of the  $W$ -nucleon collisions, is equivalent to the ‘gedanken experiment’ formula (1), summed up over the spin indices. This reference frame will be called hereafter the *collinear  $W$ -nucleon collision* frame.

We have thus demonstrated that the femto-experiment analysis framework is identical to that of the ‘gedanken experiment’. In order to measure  $s_{Wn}$  and the  $p_{out}^W$  dependence of the inclusive cross section  $\sigma_{Wn}^{incl}(p_{in}^W, p_{out}^W)$ , one has to measure the event rate  $\mathcal{N}_{evt}$ , the total flux of  $W$ -bosons  $\mathcal{F}_W(p_n, p_A, p_{in}^W | A)$ , and calculate the average target lengths  $\langle l_A(p_{in}^W, p_A) \rangle$ .

### 3.3.5 Framework for polarized $W$ -beam

In the previous sections we have proposed the framework to analyze the nucleon-nucleus collision observables in terms of the  $W$ -nucleon collision ones for the collisions of the unpolarized  $W$ -bosons assuming that the identification of the spin state of the final  $W$ -boson cannot be made. In this section we generalize this framework to describe the inclusive scattering of polarized  $W$ -bosons. Such a framework, as we shall demonstrate in the following sections, and in the forthcoming paper [1], will be very useful in exploring spin asymmetries in the collisions of the  $W$ -bosons with hadronic matter – in particular in measuring the  $W$ -nucleon collision-energy dependence of the inclusive cross-section asymmetry for longitudinally and transversely polarized  $W$ -bosons. The key point, which has triggered our interest in femto-experimenting at the LHC is that we can propose a method to tune the polarization of the  $W$ -boson beam and to measure the polarization of the outgoing  $W$ -bosons.

In Section 3.3.3 we have demonstrated that the partonic collisions producing  $W$ -bosons can be treated as a probabilistic random emission source producing the  $W$ -boson beam. For the incoherent source producing the  $W$ -bosons with the polarization  $\lambda_{in}$ , the number of events  $\mathcal{N}_{evt}^{\lambda_{in}}(p_n, p_A, p_W^{in}, p_W^{out}, p_1 | A)$  in which the  $W$ -boson produced with momentum  $p_W^{in}$  collides and changes its momentum to  $p_W^{out}$  can be

---

<sup>10</sup>The reason why we have kept the decay-topology dependent probabilities will become clear in the following section devoted to the discussion of the framework for the collisions of polarized  $W$ -boson beams.

expressed by the following formula:

$$\begin{aligned} \mathcal{N}_{evt}^{\lambda_{in}}(p_n, p_A, p_W^{in}, p_W^{out}, p_1 | A) &= \mathcal{F}_W^{\lambda_{in}}(p_n, p_A, p_W^{in} | A) \\ &\times \left| \sum_{\lambda_{out}} \mathcal{S}_{Wn}^{\lambda_{in}, \lambda_{out}}(p_W^{in}, p_W^{out}) \mathcal{D}_W^{\lambda_{out}}(p_1, p_W^{out} - p_1) \right|^2 \langle l_A(p_W^{in}, p_A) \rangle \rho_A(p_A), \end{aligned} \quad (12)$$

where  $\mathcal{F}_W^{\lambda_{in}}(p_n, p_A, p_W^{in} | A)$  is the flux of the  $W$ -bosons with the polarization  $\lambda_{in}$ ,  $\mathcal{S}_{Wn}^{\lambda_{in}, \lambda_{out}}(p_W^{in}, p_W^{out})$  is the amplitude of the  $W$ -boson scattering on a nucleon, leading to a change of its momentum to  $p_W^{out}$  and to a change of its polarization to  $\lambda_{out}$ , and  $\mathcal{D}_W^{\lambda_{out}}(p_1, p_W^{out} - p_1)$  is the decay amplitude of the  $W$ -boson into two  $SU(2)_L$ -doublet fermions.

The important property of this formula reflects the fact that the spin of the outgoing  $W$ -boson could not be directly measured, even if we were able to measure all particles produced in the nucleon–nucleus collisions. Therefore, a coherent summation over the pure spin states of the outgoing  $W$ -boson has to be made.

The relation of spin-dependent amplitudes to the  $W$ –nucleon inclusive cross section can be written as follows:

$$\int d^3p_1 \frac{\sum_{\lambda_{in}} \mathcal{F}_W^{\lambda_{in}}}{\mathcal{F}} \frac{|\sum_{\lambda_{out}} \mathcal{S}_{Wn}^{\lambda_{in}, \lambda_{out}} \mathcal{D}_W^{\lambda_{out}}|^2}{\sigma_{Wn}^{incl}} = 1. \quad (13)$$

This relation defines the units of the global normalization factor of  $\mathcal{S}$  to be the cross-section units.

The observables describing the inclusive collisions of the polarized  $W$ -bosons:  $W^{\lambda_{in}} + n \rightarrow W^{\lambda_{out}} + X$  have to be unfolded from the observed event rate. The most convenient reference frame in which such unfolding can be made is the  $W$ -boson rest frame in which the spin quantization axis is chosen to be the *collinear  $W$ –nucleon collision* frame  $z$ -axis. The spin dependent observables can be unfolded from the measured angular distribution of the  $W$ -boson decay products.

In the  $W$ -boson rest frame the number of events in which the charged lepton is emitted at the angles  $(\theta, \phi)$ , with respect to the spin quantization axis, can be expressed as follows:

$$\begin{aligned} \mathcal{N}_{evt}^{\lambda_{in}}(p_n, p_A, p_W^{in}, p_W^{out} = 0, \cos \theta, \phi | A) &= \\ \frac{3}{4\pi} \sum_{\mu, \nu} \sum_{\lambda_1, \lambda_2} \mathcal{F}_W^{\lambda_{in}}(p_n, p_A, p_W^{in} | A) \mathcal{S}_{Wn}^{\lambda_{in}, \lambda_1}(p_W^{in}, p_W^{out}) \mathcal{S}_{Wn}^{*\lambda_{in}, \lambda_2}(p_W^{in}, p_W^{out}) |\mathcal{T}^{\mu\nu}|^2 \\ &\times D_{\lambda_1(\mu-\nu)}^{1*}(\cos \theta, \phi) D_{\lambda_2(\mu-\nu)}^1(\cos \theta, \phi) \langle l_A(p_W^{in}, p_A) \rangle \rho_A(p_A), \end{aligned} \quad (14)$$

where  $\mathcal{N}_{evt}^{\lambda_{in}}$  is the total number of events having the kinematic variables  $(p_n, p_A, p_W^{in}, \cos \theta, \phi)$ ,  $\mathcal{T}^{\mu\nu}$  are the Standard Model helicity amplitudes of the decay of the  $W$ -boson into leptons having, respectively, the spins  $\mu$  and  $\nu$ ,  $D_{\lambda_2(\mu-\nu)}^1(\cos \theta, \phi)$  and  $D_{\lambda_1(\mu-\nu)}^{1*}(\cos \theta, \phi)$

are the matrices corresponding to Wigner rotations for spin-1 particles, and  $\rho_A(p_A)$  is the nucleus density in the  $W$ -rest frame.

The above formula is derived using the helicity amplitude formalism presented in Ref. [4] and expressing the spin density matrix of the outgoing  $W$ -boson as:

$$\rho_{W_{out}}^{\lambda_1, \lambda_2} = \sum_{\lambda_{in}, \lambda} \rho_W^{\lambda_{in}, \lambda} \mathcal{S}_{W_n}^{\lambda_{in}, \lambda_1}(p_W^{in}, p_W^{out}) \mathcal{S}_{W_n}^{*\lambda, \lambda_2}(p_W^{in}, p_W^{out}) \quad (15)$$

where

$$\rho_{W_{in}}^{\lambda_{in}, \lambda} = \delta^{\lambda_{in}, \lambda} \frac{\mathcal{F}_W^{\lambda_{in}}}{\sum_{\lambda_{in}} \mathcal{F}^{\lambda_{in}}}. \quad (16)$$

The full information on the amplitudes (including phases) of the polarized  $W$ -scattering is contained in the  $\mathcal{S}_{W_n}^{\lambda_1, \lambda_2}$  matrix elements. In order to measure their  $s_{W_n}$  and  $p_{out}^W$  dependence, we need to polarize the beam of  $W$ -bosons, and to measure their flux  $\mathcal{F}^{\lambda_{in}}(p_n, p_A, p_{in}^W | A)$  and the event rate  $\mathcal{N}_{evt}(p_n, p_A, p_W^{in}, p_W^{out} = 0, \cos \theta, \phi | A)$ .

### 3.4 Measuring kinematic variables at LHC

If the beam of the  $W$ -bosons at the LHC could be momentum and spin tagged, and if the momentum and spin of the outgoing  $W$ -boson could be unambiguously determined from the angular distribution of the final-state leptons, then the CMS-energy and polarization dependence of the  $W$ -nucleon cross section (polarized matrix elements) could be directly determined from the observed event rates using the above formulae<sup>11</sup>. However, at the LHC the remnants of the nucleon and of the nucleus cannot be measured<sup>12</sup>. Similarly, the momentum of the outgoing neutrino cannot be directly measured. As consequence the projected momenta of the incoming and of the outgoing  $W$ -boson on the nucleon-nucleus collision axis cannot be measured. The projected momenta of the incoming and of the outgoing  $W$ -bosons on the plane perpendicular this axis can be measured only if the final state particles can be associated either to the recoil system produced in the primary collision producing the  $W$ -boson, or to the group of particles produced in the subsequent collision of the  $W$ -boson. Note that the above two systems fragment independently and do not have any colour interconnection (their correlation and quantum interferences would be important only if the nuclear de-excitation global variables were measured). These issues will be discussed in more detail in Ref. [1] – in the following, we shall assume that an algorithm for such an association can be devised and that one can provide,

---

<sup>11</sup>The procedure of determining the inclusive polarized  $W$ -nucleon cross section would be analogous to the determination of the polarized  $\rho$ -nucleus cross section using  $e$ - $A$  collisions of polarized electron beam and tagging the initial and the final-state electron momenta and the momenta of the pions produced in the  $\rho$ -meson decays.

<sup>12</sup>The highest energy circular collider where a  $4\pi$ -detector, integrated with the machine lattice, was designed is the RHIC collider [5, 6, 7].

on the event-by-event basis, the estimators of the transverse momenta of the two systems,  $\vec{p}_T^{\text{recoil}}$  and  $\vec{p}_T^{\text{subs}}$ . The transverse momentum of the outgoing  $W$ -boson can thus be expressed as  $\vec{p}_T^{W,\text{out}} = -(\vec{p}_T^{\text{subs}} + \vec{p}_T^{\text{recoil}})$ , and the transverse momentum of the neutrino as  $\vec{p}_T^\nu = \vec{p}_T^{W,\text{out}} - \vec{p}_T^l$ .

### 3.5 Polarization of $W$ -bosons at LHC

The spin of the  $W$ -boson beam particles cannot be measured on the event-by-event basis. The  $W$ -beam can be considered as an incoherent mixture of the three beams representing the three polarization states of the  $W$ -bosons. The spin-dependent observables must thus be defined in terms of the sums of the cross sections weighted by the relative intensities of the beams with the three polarization states. The polarization of the outgoing  $W$ -boson is encoded into the angular distributions of its decay products. Since the longitudinal momentum of the outgoing  $W$ -boson cannot be measured at the LHC, the two spin-analysis angles are reduced to only one, chosen in this paper as the angle,  $\phi_l^t$ , between of the produced charged lepton and the outgoing  $W$ -boson in the plane perpendicular to the nucleon–nucleus collision axis.

### 3.6 Unfolding of $W$ –nucleon collision observables in LHC environment

At the LHC, the  $W$ –nucleon collision observables will have to be unfolded from the observed rates of events containing the final-state charged lepton (preferably electron or muon) and missing transverse energy. These events will be characterized by: the reconstructed lepton momentum  $p_l$ , the reconstructed transverse momentum of the neutrino  $\vec{p}_T^\nu$ , and the reconstructed transverse momentum of the particle system associated with the  $W$ -boson recoil system<sup>13</sup>  $\vec{p}_T^{\text{recoil}}$ .

The relationship between the rates of events containing the above leptonic sig-

---

<sup>13</sup>Other topological variables characterizing the hadronic and leptonic energy flow in selected events could be very useful for detailed studies of the mechanism of the  $W$ -boson interactions. This aspect is not discussed in this paper.



natures and the  $W$ -nucleon collision observables can be written as:

$$\begin{aligned}
\mathcal{N}_{\text{LHC}}(p_n, p_A, p_T^{\text{recoil}}, p_T^\nu, p_l | A) = & \\
& \int d^3 p_W^{\text{in}} \int d^3 p_W^{\text{out}} \delta^{(2)}(p_T^{W, \text{in}} - p_T^{\text{recoil}}) \delta^{(2)}(p_T^\nu + p_T^l - p_T^{W, \text{out}}) \\
& \times \mathcal{F}_W(p_n, p_A, p_W^{\text{in}} | A) [1 - \sigma_{\text{tot}}^{\text{abs}}(p_{\text{in}}^W) \langle l_A(p_{\text{in}}^W, p_A) \rangle \rho_A(p_A)] \\
& \times \left[ 1 - \sigma_{\text{tot}}^{\text{incl}}(p_{\text{in}}^W) \{1 - \Theta(|p_{\text{in}}^W - p_{\text{out}}^W| - \epsilon)\} \langle l_A(p_{\text{in}}^W, p_A) \rangle \rho_A(p_A) \right. \\
& \quad \left. + \sigma_{Wn}^{\text{incl}}(p_{\text{in}}^W, p_{\text{out}}^W) \Theta(|p_{\text{in}}^W - p_{\text{out}}^W| - \epsilon) \langle l_A(p_{\text{in}}^W, p_A) \rangle \rho_A(p_A) \right] \\
& \times \mathcal{P}_{\text{decay}}(p_{\text{out}}^W, p_l),
\end{aligned} \tag{17}$$

for the measurement of the total inclusive cross section, and:

$$\begin{aligned}
\mathcal{N}_{\text{LHC}}^{\text{pol}}(p_n, p_A, p_T^{\text{recoil}}, p_T^\nu, p_T^l, |p_l|, \phi_l^t | A) = & \\
\frac{3}{4\pi} \sum_{\mu, \nu} \sum_{\lambda_{\text{in}}, \lambda_1, \lambda_2} \int d^3 p_W^{\text{in}} \int d^3 p_W^{\text{out}} \delta^{(2)}(p_T^{W, \text{in}} - p_T^{\text{recoil}}) \delta^{(2)}(p_T^\nu + p_T^l - p_T^{W, \text{out}}) & \\
\times \mathcal{F}_W^{\lambda_{\text{in}}}(p_n, p_A, p_W^{\text{in}} | A) [1 - \sigma_{\text{tot}}^{\text{abs}}(p_{\text{in}}^W) \langle l_A(p_{\text{in}}^W, p_A) \rangle \rho_A(p_A)] & \\
\times \mathcal{S}_{Wn}^{\lambda_{\text{in}}, \lambda_1}(p_W^{\text{in}}, p_W^{\text{out}}) \mathcal{S}_{Wn}^{*\lambda_{\text{in}}, \lambda_2}(p_W^{\text{in}}, p_W^{\text{out}}) \langle l_A(p_{\text{in}}^W, p_A) \rangle \rho_A(p_A) & \\
\times |\mathcal{T}^{\mu\nu}|^2 D_{\lambda_1(\mu-\nu)}^{1*}(\cos \theta, \phi) D_{\lambda_2(\mu-\nu)}^1(\cos \theta, \phi) &
\end{aligned} \tag{18}$$

for the measurement of the spin dependent matrix elements<sup>14</sup>.  $\sigma_{\text{tot}}^{\text{incl}}(p_{\text{in}}^W)$  is the total inclusive cross section and the  $\sigma_{\text{tot}}^{\text{abs}}(p_{\text{in}}^W)$  is the  $W$ -boson absorption cross section. The symbol  $\delta^{(2)}(x)$  represents the 2-dimensional Dirac  $\delta$ -function, and  $\Theta(x)$  represents the step function:  $\Theta(x) = 0$  for  $x < 0$ , and  $\Theta(x) = 1$  for  $x \geq 0$ . All  $p_T$ s in the above formulae are 2-dimensional vectors in the transverse momentum plane, while other  $p$ s denote three-momenta. The introduction of the  $\Theta(x)$  function and its parameter  $\epsilon$  is technical. It allows to define the two origins of the observed events: those in which the outgoing  $W$ -bosons interacted in the hadronic matter and those in which they did not. Such a separation is not physical. The measurement results must not depend upon the way how these subsamples are defined. Indeed, the  $\epsilon$  dependence of the sum of the two corresponding terms vanishes, in any concrete unfolding procedure, as soon as the  $\epsilon$  value is chosen to be smaller than the resolution with which the sum of the transverse momenta,  $\vec{p}_T^{\text{recoil}} + \vec{p}_T^\nu + \vec{p}_T^l$ , is measured<sup>15</sup>. The term  $[1 - \sigma_{\text{tot}}^{\text{abs}}(p_{\text{in}}^W) \langle l_A(p_{\text{in}}^W, p_A) \rangle \rho_A(p_A)]$  describes the disappearance of the  $W$ -bosons.

<sup>14</sup>The angles  $\theta$  and  $\phi$  in eq. (18) are expressed in terms of  $p_W^{\text{out}}$ ,  $p_T^l$ ,  $|p_l|$  and  $\phi_l^t$ .

<sup>15</sup>For the spin-dependent formula the technical separation is not necessary because  $\mathcal{S}^{\lambda_1, \lambda_2}$  contains both contributions, whatever criteria of the technical splitting of the full sample of events into the transmission and interaction subsamples are used.

The precision of unfolding of the  $W$ -nucleon collision observables will be driven by the statistical precision of measuring event rates and by the systematic precision of measuring the kinematic variables. However, the most important source of the measurement errors will be the uncertainties in the kernels of the integral equations. The quest for their high precision is amplified not only by the fact that only the integrated rates will be measured at the LHC, but also by the fact that in the Monte-Carlo-based unfolding methods, the propagation of the kernel errors to the measured quantity cannot be fully controlled.

The kernels of the integral equation contain the expressions which can be precisely calculated and those which depend upon the external experimental input. The dominant contribution to a measurement error will be due to the uncertainty in the kinematic, spin and nuclear dependence of the flux of the  $W$ -bosons<sup>16</sup>,  $\mathcal{F}_W^{\lambda_{in}}(p_n, p_A, p_W^{in}|A)$  and the  $W$ -boson momentum dependence of the average target length. The precision with which they could be presently calculated will likely turn out to be insufficient to explore the rare collision of  $W$ -bosons. Therefore one has to propose special measurement procedures reducing the influence of these uncertainties on the measurement of the  $W$ -nucleon collisions observables. In the following section of this paper we shall propose such procedures fulfilling the third, necessary and sufficient condition, which must be satisfied for “configuring” the nucleon–nucleus collisions at the LHC as the femto-experiment for the investigation of the high-energy  $W$ -bosons interactions with matter.

## 4 Beams

### 4.1 Theoretical control

The  $W$ -boson beams will be generated, at the Interaction Points (IPs) of the LHC collider, by hard collisions of the constituents of the colliding particles: quarks, antiquarks and gluons. The leading process is the Drell–Yan-like annihilation of quarks and antiquarks – the members of  $SU(2)_L$  doublets with opposite values of the third weak-isospin component. Non-diagonal elements of the Cabbibo-Kobayashi-Maskawa (CKM) matrix lead to mixing between the quark generations. The  $W$ -bosons do not couple directly to gluons. However, gluons can couple to a quark–antiquark pair, providing a supplementary source of quarks and antiquarks for the Drell–Yan-like process. This latter process, even if next-to-leading in the strong interaction coupling constant  $\alpha_s$ , influences considerably the  $W$  production rates at the LHC since the high energies of the colliding beams allow to reach the low Bjorken- $x$  region where the gluon density in the nucleon becomes sizeable.

---

<sup>16</sup>Note that, conceptually, the unfolding methods for the  $W$ -beam fluxes at the LHC will be similar to those developed in the past for the SPS neutrino fluxes.

The cross section of the  $W$ -boson production at hadronic colliders is calculated as a product of the hard scattering cross section and parton distribution functions (PDFs). The hard scattering cross section can be calculated using perturbative methods with the precision of  $\mathcal{O}(\alpha_s^2)$  at the high transverse momentum of the  $W$ -boson [8]. For the transverse momentum of the  $W$ -boson substantially smaller than its mass, the fixed order perturbative result has to be complemented by a re-summation of large logarithmic correction to all orders in  $\alpha_s$  [9].

The electroweak radiative cross sections modify the calculated cross section with terms proportional to  $\alpha_{QED}$ . Contrary to the QCD corrections, they depend upon the flavour of produced leptons. The electroweak radiative corrections are dominated by the virtual corrections to  $W$ -propagator and vertices and by the QED radiation by the final state lepton(s) [10, 11]. The photon radiation from the quarks, the interference terms as well as higher-order radiative corrections, including re-summation of multiple soft-photon emissions, must also be included in high-precision calculations [10, 11, 12].

By the time when the LHC will start taking data the  $W$  production processes are expected to be controlled theoretically to  $\sim 1$ –2% for fixed PDFs. The detailed discussion of theoretical and experimental aspects of the  $W$ -boson production in hadronic colliders can be found e.g. in Ref. [13], and recently in Ref. [14].

The presently known QCD calculation methods do not allow the PDFs to be directly calculated. The perturbative methods allow, however, to derive the relevant PDFs from the deep-inelastic scattering data and to extrapolate them to the virtualities scales involved in  $W$ -boson production. Uncertainties of the PDFs arising from various theoretical sources have been propagated to the uncertainties in the predicted  $W$ -production cross section in Ref. [15]. The uncertainty of the PDFs will determine the precision of the predicted  $W$ -production cross sections at the LHC, and its rapidity and transverse-momentum dependence. The  $W$ -production cross section for the  $p$ – $p$  collision will likely be controlled to the  $\sim 5\%$  precision at the start-up of the LHC operation. This uncertainty will be gradually diminished with increasing global understanding of the LHC data.

The nuclear PDFs suffer from large uncertainties, in particular in the small- $x$  domain where only fixed-target deep-inelastic scattering data, confined to low-virtuality scales, are available for the QCD fits. The extrapolation of these data to the LHC virtuality scales must involve, at present, modeling of static nuclear effects, which are not controlled by the perturbative QCD.

## 4.2 Monte Carlo event generator

The complexity of the interplay of the QCD and QED radiation and sophisticated experimental procedures to derive  $W$ -boson fluxes from the LHC data requires a dedicated Monte Carlo event generator. The ultimate Monte Carlo generator should,

ideally, include the full set of QCD and electroweak radiative corrections, re-summed in the phase-space regions where emission of soft radiation quanta is abundant, the phenomenological parameterizations of non-perturbative effects, such as the intrinsic transverse momentum of partons. It should be based upon the most precise PDFs for nucleons and nuclei. Such a Monte Carlo generator is being developed at the moment, see e.g. [12, 16, 17, 18, 19].

In the present study we use its present development version, the Monte Carlo event generator **WINHAC** [12, 20]. At the present development stage, this generator incorporates only the leading-order process of creation of  $W$ -bosons, but includes already the EW radiative corrections in leptonic  $W$  decays. More precisely, collinear configurations of initial quarks are generated from the PDFs, while the perturbative QCD effects are included through appropriate scaling violation. All  $W$ -bosons produced by the present generator have  $p_T^W = 0$ . A set of PDF parameterizations is provided through the **PDFLIB** package [21].

Since, at hadron colliders, the  $W$ -bosons can be identified efficiently only through their leptonic-decay channels, only leptonic decays are currently implemented in **WINHAC**. The process of leptonic  $W$  decays is described within the framework of the Yennie–Frautschi–Suura exclusive exponentiation [22], where all the infrared QED effects are re-summed to the infinite order. The residual non-infrared EW corrections are calculated perturbatively. In the current version of the program the latter corrections are included up to  $\mathcal{O}(\alpha)$ . **WINHAC** went successfully through several numerical tests [12], and was also cross-checked with the independent Monte Carlo program **HORACE** [23].

The unique merit of the **WINHAC** event generator, for the studies discussed in this paper, is that the  $W$  production and decay processes are described using the spin amplitude formalism. The spin amplitudes for the  $W$  production and the  $W$  decay are calculated separately. They correspond to all possible spin configurations of the intermediate  $W$ -boson, and of the initial and final-state fermions. The matrix element for the charged-current Drell–Yan process is obtained by summing the production and decay amplitudes over the intermediate- $W$  spin states. The amplitudes are evaluated numerically for given particles four-momenta and polarizations. They can be calculated in any Lorentz frame in which the corresponding particles four-momenta are defined. For more detailed discussion see Ref. [12]. The advantage of using the spin amplitudes is that one can control the spin states, in particular the production of longitudinally and transversely polarized  $W$ -bosons. Within this formalism one can also include easily the effects of collisions of the  $W$ -boson in hadronic matter assuring the coherence of the mixed states of the  $W$ -bosons throughout the collision and decay phases.

This Monte Carlo program allows to provide a first glimpse on the spectra and polarization of produced  $W$ -bosons, also in the presence of realistic experimental event selections. While the overall longitudinal spectra of  $W$ s are well controlled,

the current version of the program does not provide information on their transverse spectra. The latter can be described realistically by initial-state parton shower algorithms, possibly matched with the NLO contributions to the hard process. This will be worked out further in Refs. [17, 18, 19].

The partonic distributions for the proton are taken from the PDFLIB package – in our studies we used the MRS (G) parametrization (Ngroup=3 and Nset=41 in the PDFLIB notation [21]). The partonic distributions for ion beams are also taken from PDFLIB. They include the nuclear shadowing effects parametrized by the EKS group [24]. This parametrization is based upon the DGLAP extrapolation of the nuclear targets DIS data to the hardness scale of the  $W$ -boson production, and upon a phenomenological modeling of the static nuclear effects.

## 4.3 Fluxes

### 4.3.1 Beam momentum spectra

The WINHAC predictions for the fluxes of the  $W$ -bosons  $\mathcal{F}_W(p_n, p_A, p_W^{in}|A)$  produced in four LHC collision schemes:  $p$ - $p$ ,  $p$ - $Pb$ ,  $D$ - $Pb$ , and  $D$ - $Ca$  (where  $D$  denotes deuteron) are shown in Fig. 3. The fluxes are plotted as a function of the logarithm of the  $W$ -boson momentum,  $|p_W^{in}|$ , measured in the collinear  $W$ -nucleon collision frame defined in Section 3.3.4.

The energies of primary beams satisfy the equal magnetic rigidity condition:

$$E_{\text{beam}} = 7 \frac{Z}{A} \text{ TeV}, \quad (19)$$

where  $Z$  and  $A$  are, respectively, the ion charge and its atomic number. These plots are normalized using the design luminosity for the  $pp$  scattering:  $L_{pp} = 10^{34} \text{ cm}^{-2} \text{ s}^{-1}$ . We have assumed the following scaling of the luminosity with the atomic numbers  $A_1$  and  $A_2$  of the primary beams:

$$L_{A_1 A_2} = \frac{L_{pp}}{A_1 A_2}. \quad (20)$$

Such an assumption is realistic for collisions in which one of the colliding beam has a very small  $A$ . In such a case the beam-beam luminosity limits are less important than the limits driven by the bunch parameters, and by their collision frequency. In addition such a scaling is practical for studying the collisions of the point-like constituents of the beam particles. The luminosity scaled according to eq. (20) assures the  $A$ -independent luminosity of the parton-parton collisions in the limit of a dilute gas of partonic clouds.

The fluxes of the beam particles vary in the range from 200 ( $p$ - $Pb$ ) to 370 ( $p$ - $p$ )  $W$ -bosons per second. It is interesting to note that these fluxes are similar to the

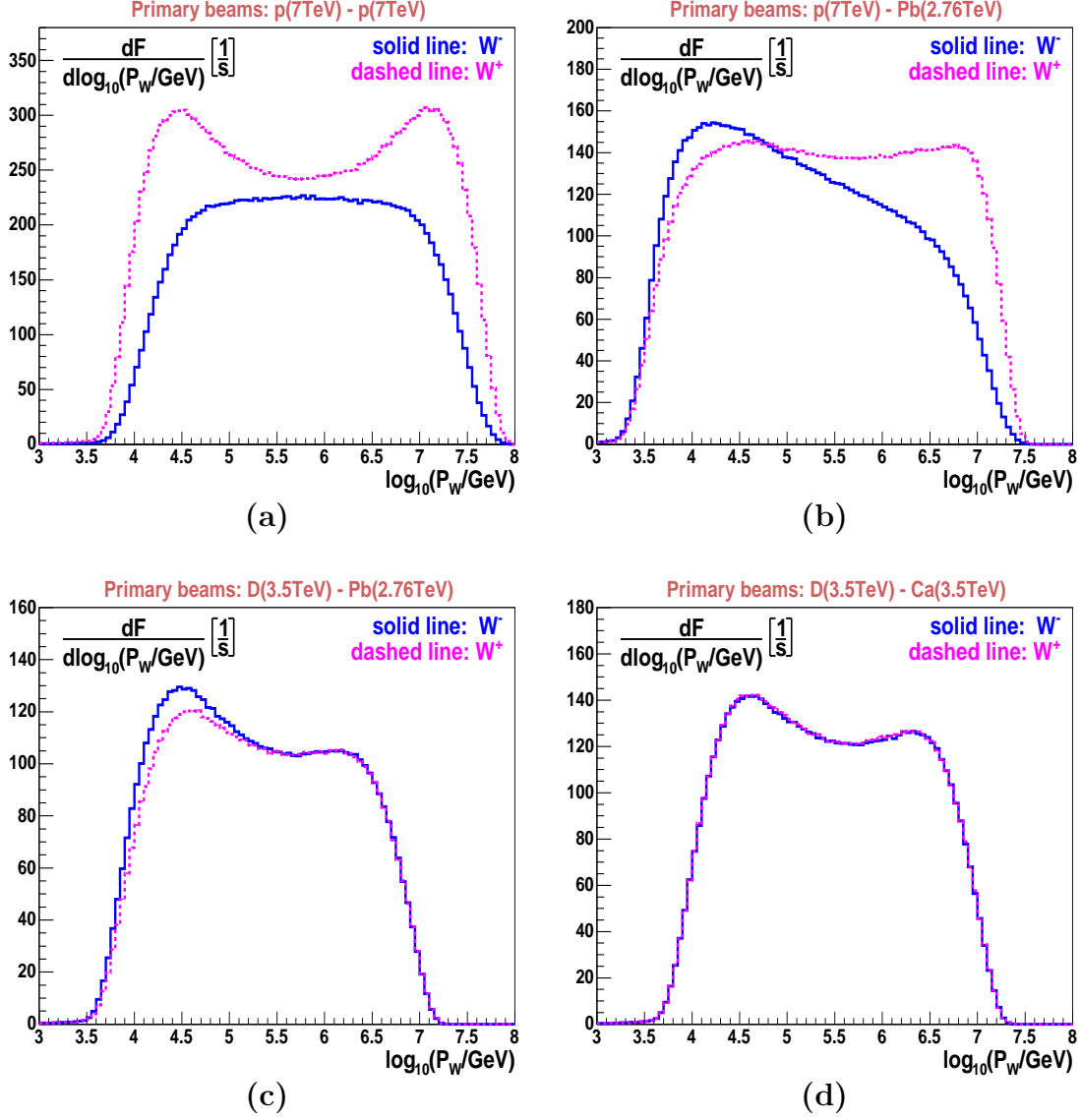


Figure 3: The fluxes of the  $W^+$  and  $W^-$  beams for the collisions of: (a)  $p$ - $p$ , (b)  $p$ - $\text{Pb}$ , (c)  $\text{D}$ - $\text{Pb}$  and (d)  $\text{D}$ - $\text{Ca}$ , for the luminosity of the primary collisions:  $L_{A_1 A_2} = 10^{34}/(A_1 A_2) [\text{cm}^{-2} \text{s}^{-1}]$ , as a function of the  $W$ -boson momentum in the collinear  $W$ -nucleon collision frame .

fluxes of secondary hadrons used in the in the first bubble-chamber experiments at CERN. The beam is a Wide-Momentum-Band beam. Its momentum spectrum extends over four orders of magnitude, from 10 TeV to 100 PeV,

The momentum distribution of the  $W$ -bosons produced in proton–proton collisions, shown in Fig. 3a, exhibits an asymmetry of the spectra of positively and negatively charged  $W$ -bosons. This is a direct consequence of a net excess of the  $u$ -quarks with respect to the  $d$ -quarks. It is particularly large in the small and in the large  $\log_{10} |p_W^{in}|$  regions, where the  $W$ -bosons are produced mostly in the collisions of the valence quarks of the incoming beam particles. The charge asymmetry reflects directly the ratio of the  $d$ -quark and the  $u$ -quark densities in this region. The momentum distribution of the  $W$ -boson flux in the proton–lead collisions is shown in Fig. 3b. The charge asymmetry changes sign for the “small”-momentum  $W$ -bosons due to the excess of neutrons over protons in heavy ions and the corresponding excess of the  $d$ -quarks over the  $u$ -quarks. It disappears partially, as illustrated in Fig. 3c, for the deuteron–lead collisions (in the large  $\log_{10} |p_W^{in}|$  domain) and completely, as illustrated in Fig. 3d, for the deuteron–calcium collisions.

The size of the nuclear effects in partonic distributions (departure from a dilute-gas approximation) is illustrated in Fig. 3d, where the momentum distribution of the  $W$ -boson flux is plotted for the primary collisions of iso-scalar beams having equal number of the  $d$  and  $u$ -quarks. The asymmetry of the low-momentum part and the high momentum part reflects the asymmetry in the nuclear corrections of the two beam particles. This collision configuration is particularly interesting and will be discussed in detail in the forthcoming paper [1]. In this configuration the fluxes of the  $W$ -bosons and those of the  $Z$ -bosons can be directly related to each other.

The above plots illustrate the dynamic range in which the momentum spectrum of the  $W$ -beam can be tuned at the LHC. The knobs for such a tuning are: the choice of the atomic numbers of colliding particles, and the selection of the charge of the  $W$ -boson. Such a tuning capacity, together with the capacity of tuning the energies of primary beams will play an important role in controlling the precision of unfolding the  $W$ -collision observables<sup>17</sup>. The studies of internal consistency of the momentum spectra for the positive and for negative  $W$ -bosons for variable atomic number of the primary beams will be of important help in scrutinizing independently the PDFs (both for the valence and the sea quarks) and the effects driving the energy dependence of the partonic emittance.

---

<sup>17</sup>We would like to recall that varying the momentum byte and the relative proportion of the pions and kaons generating the neutrino beams for the SPS neutrino collision program was indispensable for precise measurements of the neutrino–nucleon and antineutrino–nucleon cross sections [25, 26].

### 4.3.2 Polarization

For the studies of collisions of the  $W$ -boson with the nucleon the natural choice of the spin quantization axis is the  $z$ -axis of the *collinear  $W$ -nucleon collision frame* defined in Section 3.3.4. In this reference frame the spin direction of the longitudinally polarized  $W$ -boson is perpendicular to the  $W$ -nucleon collision axis.

The polarization of the  $W$ -beam is a direct consequence of the  $V - A$  coupling of the  $W$ -boson to quarks. If quarks were massless and if they moved collinearly with their parent hadrons then the  $W$ -bosons would only be transversely polarized. The relative proportion of the  $\lambda = +1$  and the  $\lambda = -1$  fluxes would reflect the probability of the incoming quark to move along the  $-z$  or  $+z$  direction. Longitudinally polarized  $W$ -bosons ( $\lambda = 0$ ) are produced in the process of annihilation of massive quark(s) and/or in the annihilation of the quarks which are not collinear with their parent hadrons. The relevant experimental observable which allows to tune the relative fluxes of the transversely and longitudinally polarized  $W$ -bosons is the transverse momentum,  $p_T^{\text{recoil}}$ , of the recoiled particles in the  $W$ -production process.

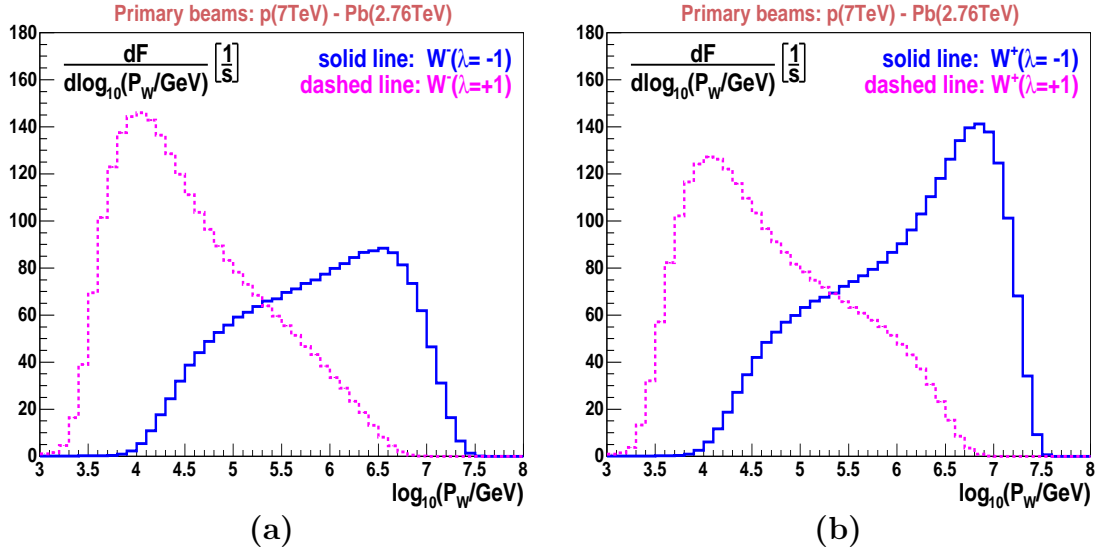


Figure 4: The fluxes of the transversely polarized  $W$ -beams.

In Fig. 4 we show the WINHAC predictions for the polarization dependence of the  $W$ -boson beam fluxes:  $\mathcal{F}_W^{\lambda_{in}}(p_n, p_A, p_W^{in}|A)$ , for the primary collisions of the proton and the lead-ion beams. The fluxes are plotted as a function of the beam momentum, separately for the beams of the positively and the negatively charged  $W$ -bosons.. At the lowest momentum the  $W$ -beam has purely the  $\lambda = +1$  polarization while at



the highest one it has the  $\lambda = -1$  polarization. The relative proportion of the  $\mathcal{F}_W^1$  and  $\mathcal{F}_W^{-1}$  changes monotonically with the  $W$ -beam momentum. This plot illustrates the capacity of tuning the relative proportion of the  $\lambda = +1$  and the  $\lambda = -1$  fluxes within the full dynamical range by choosing the appropriate momenta of the primary beams and, to a certain degree, by choosing the charge of the beam particles.

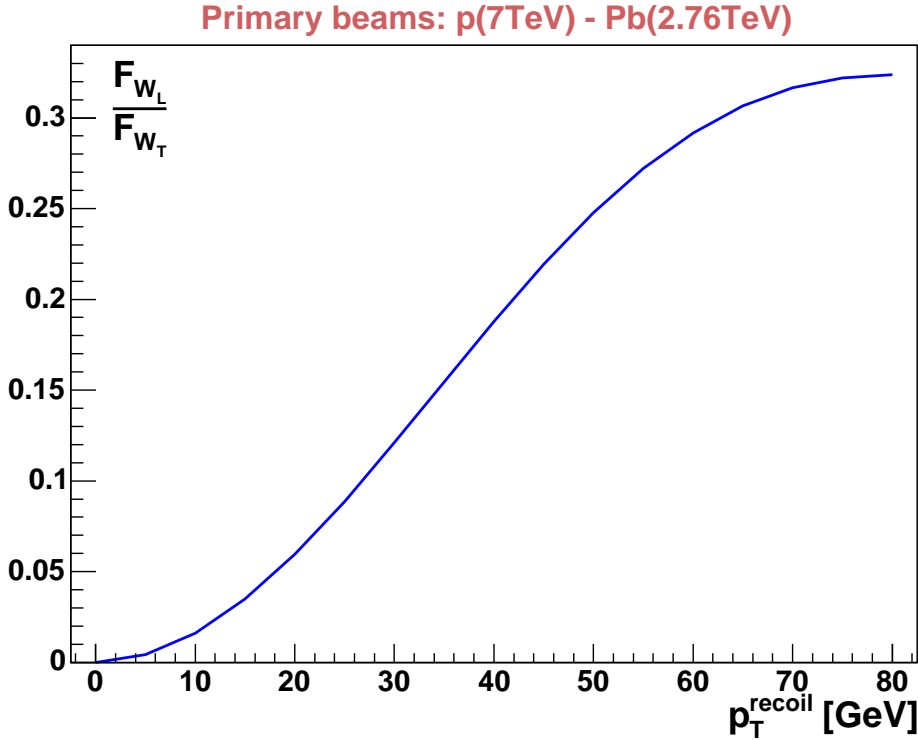


Figure 5: The relative flux of the longitudinally and transversely polarized  $W$ -bosons as a function of the  $W$ -boson recoil transverse momentum.

In the present version of WINHAC the NLO QCD processes generating the transverse momenta of partons are not included. For the preliminary estimation of the  $p_T^{\text{recoil}}$  dependence of the ratio of the fluxes of longitudinally and transversely polarized  $W$ -bosons the effect of the transverse momentum of incoming partons was emulated using the following kinematic model. The transverse momentum of the  $W$ -boson was generated randomly and attributed with equal probability to the quark (antiquark) of the nucleus and to the antiquark (quark) of the nucleon. Since the quantization axis in the  $W$ -boson rest frame points to the direction of the nucleus, the  $W$ -boson may have, in this reference frame, the longitudinal polarization only if the transverse momentum is attributed to the quark (antiquark) of the nucleus. The ratio of the fluxes of the longitudinally and transversely polarized  $W$ -bosons

was determined using the value of the Wigner rotation angle – the angle between the momentum vectors of the nucleus and of the quark in the rest frame of the  $W$ -boson. The estimated ratio is shown in Fig. 5. This plot illustrates the correlation between the transverse momentum of the  $W$ -boson recoil particles and the relative proportion of fluxes. Such a correlation allows to tune the relative intensity of the longitudinally and transversely polarized  $W$ -beams.

#### 4.4 Experimental control of fluxes – outlook

The precision of controlling the fluxes of the  $W$ -bosons at the LHC will be gradually improved, before the start-up of the LHC operation, by matching the progress in detailed understanding of the Tevatron  $W$ -production data with the increasing precision of theoretical calculation of the  $W$ -production processes. The ultimate precision which will be achieved on the “D-day” of the start-up of the LHC operation will, however, very likely be insufficient for scrutinizing the collisions of weakly interacting particles with hadronic matter. Therefore, one needs to develop dedicated measurement methods allowing to reduce the influence of the  $W$ -boson flux uncertainty on the  $W$ -boson collision observables.

Depending on the required level of sensitivity to the  $W$ -beam collision effects the following three methods of handling the  $W$ -boson fluxes are proposed in this paper:

- *the calculated flux method,*
- *the extrapolated flux method,*
- *the flux-independent method.*

The first method uses the calculated fluxes of the  $W$ -bosons. Initially, at the start-up of the LHC operation, its sensitivity to the  $W$ -collision effects will be poor due to the  $W$ -flux shape and normalization uncertainties. The main effort will have to be focused on diminishing the uncertainties in the non-perturbative inputs for the theoretical calculation of the  $W$ -fluxes: in the PDFs, and in the extrapolation of the transverse emittance of partons to the LHC collision energy. The progress will most likely be driven by studies of the spectra of leptons produced in collisions of the LHC beams.

A high-precision scrutinizing of the PDFs could profit from the parasitic LHC electron beam, proposed recently in Ref. [27], to map the partonic distributions at the LHC. If such a beam is delivered to the LHC interaction points, then the proton and the neutron PDFs could be mapped using the LHC detectors. Simultaneous measurements of the electron–proton(nucleus) collision and the proton–proton(nucleus) collisions could drastically diminish the QCD-extrapolation and normalization uncertainties. The parasitic electron beam proposed in Ref. [27] cannot, however be used to map the nuclear effects in the PDFs. These effects could be

precisely measured at the HERA collider<sup>18</sup>. If not measured at HERA, the PDFs of the nuclear bunches of quarks and gluons will thus rely on the scarce data and uncertain extrapolations – until the eRHIC program will map them [30].

In the second, *extrapolated flux* method an emphasis is put on understanding the variation of the  $W$ -boson fluxes with the atomic number of the beam particles, and on confining, as much as possible, the dominant theoretical uncertainties of predicted  $W$ -boson fluxes within the normalization factor – the  $A$ -independent, *dilute partonic system* flux. Since the nuclear size ( $A$ -dependent) effects are present both in the  $W$ -boson fluxes and in the average path-length of the  $W$ -boson in hadronic matter they cannot in be resolved by measuring only the  $A$ -dependence of the  $W$ -boson production rates. In the proposed method the fluxes of the  $W$ -bosons are determined by measuring and fitting the  $A$ -dependence of the spectra of the charged lepton in the  $\log |p_t|$  bins in the *monitoring regions*. The monitoring region is defined by choosing: the energies of the primary beams, the momentum of the  $W$ -boson, and its polarization, such that both the absorption and the inclusive cross sections for  $W$ -nucleon collisions are negligible (e.g. for transversely polarized  $W$ -bosons at low  $W$ -nucleon CMS energies).

The fluxes of the  $W$ -bosons and their polarization can be determined in the monitoring regions by measuring the angular distribution of the  $W$ -boson decay products. The observed  $A$ -dependence of the fluxes can subsequently be used in unfolding the  $W$ -boson collision effects in a configuration where they become significant. Such a procedure allows to *factorize-out* and neglect a large fraction of theoretical uncertainties of the  $W$ -fluxes. It could be employed in experimental scrutinizing of the centre-of-mass energy dependence of the cross-section for collisions of the longitudinally polarized  $W$ -bosons at the LHC-collider energies.

The precision of such a procedure is illustrated in Fig. 6. The  $A$ -dependence of the  $W$ -boson flux is fitted in the monitoring region using the rates of the events containing the  $W$ -boson decay signatures in the  $p$ - $He$ ,  $p$ - $O$ ,  $p$ - $Ca$ ,  $p$ - $Xe$  and  $p$ - $Pb$  collisions. The following form of the fit was chosen<sup>19</sup>:

$$\frac{\mathcal{F}_W}{A} = \mathcal{F}_0 \left( 1 - \alpha A^{\frac{1}{3}} \right). \quad (21)$$

We have assumed that the point to point systematic normalization errors of the rates will be kept below 2% and the  $A$ -dependent acceptance corrections will be kept below 1%. Such a precision can be achieved already in the initial period of the LHC operation. The slope of the fit is determined, with the precision of 10%, no matter what theoretical precision of the overall normalization of the *dilute partonic system flux*,  $\mathcal{F}_0$ , can be achieved.

---

<sup>18</sup>The nuclear program for the HERA collider was developed and proposed in 1997 to the HERA community as an alternative to the high-luminosity upgrade [28, 29].

<sup>19</sup>This is the simplest form of the fit which includes the effects of shadowing for the large momenta of the  $W$ -bosons ( $\alpha \geq 0$ ), and the EMC effect for the small momenta of the  $W$ -bosons ( $\alpha \leq 0$ ).

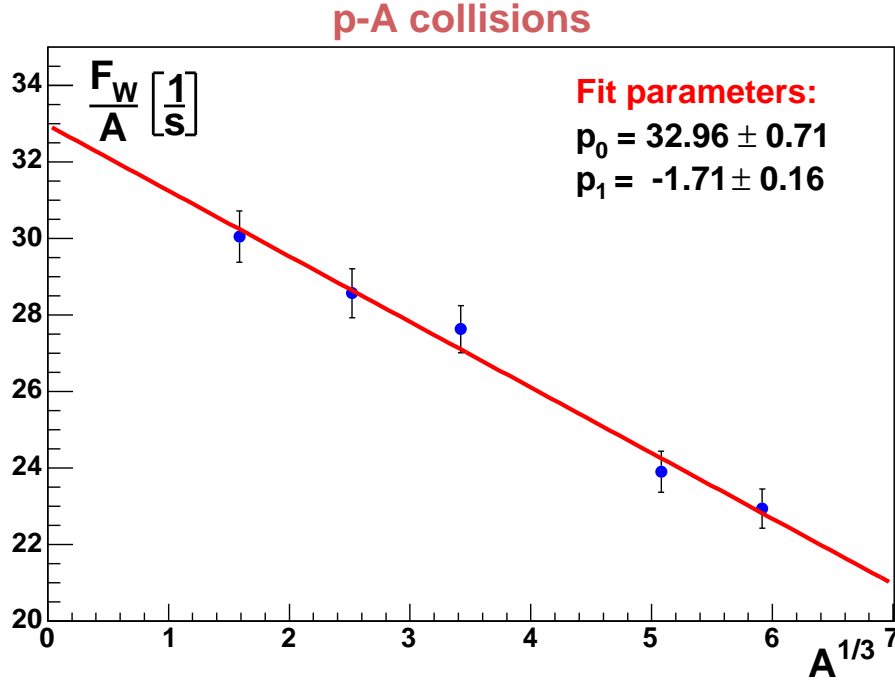


Figure 6: The fit of the  $A$ -dependence of the  $W$ -boson fluxes.

The key point of the above method is that only the relative point-to-point systematic errors are important in the fit of the  $A$ -dependence of the fluxes. Since the precision of the relative measurement of the  $W$ -boson fluxes could be significantly improved in a dedicated machine configuration, e.g. by storing simultaneously or by frequent switching between various iso-scalar nuclear beams, this method has the potential to be very precise. In the dedicated LHC running program with several ion beams a  $\sim 1\%$  sensitivity to the  $W$ -collision effects may be achieved in this method.

The third, *flux-independent* method minimizes the impact of the uncertainties in the  $W$ -boson flux for specially designed dedicated measurements. In this method, the effects of propagation of the  $W$ -bosons in hadronic matter are related to the effects of propagation of other particles. For example, the collisions of the  $W$ -bosons in hadronic matter can be monitored using the monitoring sample of the  $Z$ -bosons. For the collisions of iso-scalar nuclei (e.g. deuteron–calcium collisions), for which the differences in the momentum distribution of the  $d$ -quark and the  $u$ -quark are negligible, the uncertainty of relative fluxes of the  $W$  and  $Z$ -bosons can be reduced down to the tiny effects due to their mass difference. In this collision configuration even a very small ( $\leq 0.1\%$ ) anomalous effects in the propagation of  $W$ -bosons can be detected by using the  $Z$ -boson templates. This method will be discussed in more

detail in the forthcoming paper [1].

## 5 Targets

### 5.1 Covariant and invariant quantities

In the framework presented in Section 3 the  $W$ -boson beam targets are described by two functions: the average path of the  $W$ -boson in hadronic matter,  $\langle l_A(p_W^{in}, p_A) \rangle$ , and the nuclear density,  $\rho_A(p_A)$ . In order to preserve the Lorentz-covariance of the formulae we have kept explicitly their dependence upon the momentum of the nucleus, allowing for the apparent deformations of its volume and density in reference frames where the nucleus moves with high velocity (e.g. in the  $W$ -boson rest frame). The discussion of the control of the  $W$ -boson targets, presented in this section, uses explicitly the fact that the product of these two functions is invariant with respect to Lorentz transformations. This is because the dependence of the nucleus density and of the effective path-length of the  $W$ -boson upon the  $\gamma$ -factor of the Lorentz boost cancel each other for spherically symmetric nuclei. This allows us to discuss the effective target length in the most convenient reference frame and use the formulas derived in this frame in arbitrary Lorentz reference frame, provided that it will appear in the expressions together with the nuclear density. The most convenient reference frame is the rest frame of the nucleus with the  $z$ -direction collinear with the direction of the incoming nucleon.

### 5.2 $W$ -boson path-length

The  $W$ -boson path-length in hadronic matter is determined by the relative position of the  $W$ -boson creation cell with respect to the centre of the nucleus and by the  $W$ -boson momentum. The target length for the  $W$ -boson beam will thus vary on event-by-event basis. The event-by-event variation of the target length cannot be controlled experimentally at the LHC<sup>20</sup>. What can be controlled experimentally is the  $A$ -dependent average path-length of the  $W$ -boson in the nucleus of the atomic number  $A$ . Since the nucleus-rest-frame  $W$ -boson momentum reaches the TeV–PeV range, the observer traveling with the  $W$ -boson, views the nucleus as a “macroscopic” classical object. The quantum fluctuations of its degrees of freedom are frozen during the passage of the  $W$ -particle allowing to describe the nucleus only in terms static nuclear parameters.

In Section 3 we have implicitly assumed, that the nucleon collides with the nucleus at the impact parameter  $b = (b_x, b_y) = (0, 0)$ . The generalization of the

---

<sup>20</sup>At the LHC, wounded nucleons of the nucleus are emitted at small angles and cannot be detected.

formula (9) defining the average path-length to the case where the nucleon arrives at the position of the nucleus with the uniformly distributed impact parameter is straightforward:

$$\begin{aligned} \langle l_A(p_{in}^W) \rangle = & \int db_x \int db_y \int dx_p \int dy_p \int dz_p l(x_p, y_p, z_p, p_{in}^W | A) \\ & \times \mathcal{P}_W(x_p, y_p, z_p, b_x, b_y, p_{in}^W | A), \end{aligned} \quad (22)$$

where  $l(x_p, y_p, z_p, p_{in}^W | A)$  is the distance over which the  $W$ -boson produced with the momentum  $p_{in}^W$  travels before leaving the nucleus of the atomic number  $A$ . The above formula is general but unpractical. In the following we shall simplify it and write it in a form which will allow us to express the average path of the  $W$ -bosons in terms of quantities which can be controlled experimentally.

Firstly, we recall that the quark (antiquark) of the nucleon projectile can be localized within the transverse distances of  $L_t = 2R_n$ , where  $R_n$  is the nucleon radius<sup>21</sup>. The antiquark (quark) of the target nucleus can be localized within the transverse distances of  $L_t = 2R_A$ , where  $R_A$  is the nucleus radius. The transverse size of the  $W$ -boson formation cell (i.e. the region where, for given  $x_A$  and  $x_N$ , the  $W$ -formation process is confined) is determined by the overlap of the localization volumes of the quark (antiquark) of the nucleon and antiquark (quark) the of the nucleus. The transverse position of the  $W$ -production cell is thus restricted to the region specified by the following boundaries:  $b_x - R_n \leq x_p \leq b_x + R_n$ , and  $b_y - R_n \leq y_p \leq b_y + R_n$ . These conditions define the impact parameter and the  $W$ -boson momentum-dependent region in which the integration over  $x_p, y_p$  will have to be performed. Since the transverse-size boundary is confined to small distances (with respect to the nucleus size and the  $W$ -boson path-length), the integrals over  $x_p, y_p$  can be calculated explicitly:

$$\langle l_A(p_{in}^W) \rangle = \int db_x \int db_y \int dz_p l(b_x, b_y, z_p, p_{in}^W | A) \mathcal{P}_W(b_x, b_y, z_p, p_{in}^W | A). \quad (23)$$

Secondly, we note that the transverse momentum of the  $W$ -bosons is, for the LHC energies, significantly smaller than its nucleus-rest-frame longitudinal momentum. This allows us to ignore, in the calculation of the average path-length, the contribution coming from non-collinear  $W$ -nucleus collisions. Technically, this simplification assures the cylindrical symmetry of the integral, allowing to factorize the transverse and the longitudinal degrees of freedom. In addition, it allows us to drop the dependence upon the incoming  $W$ -boson momentum  $p_{in}^W$  in the path-length term and upon the transverse momentum of the  $W$ -boson in the probability term.

---

<sup>21</sup>The contribution of diffractive, very small momentum-transfer  $W$ -production ( $\sqrt{t} \leq R_n/2$ ) can be safely neglected here.

This simplification results in the following expression:

$$\langle l_A(p_{in}^W) \rangle = \int db_x \int db_y \rho_A^n(b_x, b_y) \int dz_p \mathcal{P}_W^b(z_p(p_{in}^W)) l(b_x, b_y, z_p | A), \quad (24)$$

where  $\rho_A^n(b_x, b_y)$  is the transverse density of nucleons in the nucleus, normalized to the integrated transverse density. The  $\mathcal{P}_W^b$  is the probability of forming the  $W$ -boson at the longitudinal distance  $z_p(p_{in}^W)$  with respect to the position of the centre of the nucleus for the fixed-impact-parameter nucleon–nucleus collision. Its explicit calculation requires the experimental knowledge of space-distribution (both in the impact parameter and in the longitudinal distance) of the quarks (antiquarks) involved in the production of the  $W$ -boson. The precise determination of the impact parameter dependence of the PDFs was the principal goal of the nuclear program for HERA [28, 29] and remains one of the target of the future eRHIC experimental program at the BNL [30]. Before such measurements are made, the average path-length of the  $W$ -bosons can be controlled precisely only in the kinematic domains where the knowledge of the space-distribution of partons is not indispensable.

### 5.3 Effective targets for $W$ -beam

For the  $W$ -bosons produced at small momenta in asymmetric collisions of small- $x$  parton from the nucleon and large- $x$  parton from the nucleus, the size of the  $W$ -boson formation cell:

$$L_l(x_A) = \frac{1}{x_A M_A} \leq 2R_n \quad (25)$$

is small and the integrals in eq. (24) can be calculated independently of the exact form of the  $\mathcal{P}_W^b$ . This is because the  $W$ -boson formation cell is, in such a case, localized both transversally and longitudinally within the volume of individual nucleons, and the total  $W$ -boson path-length in nuclear matter is independent of the exact position of the  $W$ -boson creation point. In this region  $\langle l_A(p_{in}^W) \rangle$  is independent of the  $W$ -boson momentum and can be expressed as:

$$\langle l_A \rangle = \int db_x \int db_y \rho_A^n(b_x, b_y) \int dz_p \frac{\sqrt{R_A^2 - b_x^2 - b_y^2 - z_p}}{2\sqrt{R_A^2 - b_x^2 - b_y^2}}, \quad (26)$$

where  $R_A$  is the nucleus radius. This universal atomic-number-dependent quantity representing the average target length for the  $W$ -bosons formed by the large- $x_A$  parton of the nucleus defines the *effective target length* for the  $W$ -boson beam. It can be tuned by choosing the atomic number of the LHC ion beam<sup>22</sup>.

---

<sup>22</sup>In the general case of an arbitrary Ioffe length the average path-length is a function of the CMS energy of the  $W$ -nucleon collisions  $s_{Wn}$  and can be written as:  $\langle l_A(s_{Wn}) \rangle = K(s_{Wn}) \langle l_A \rangle$ ,

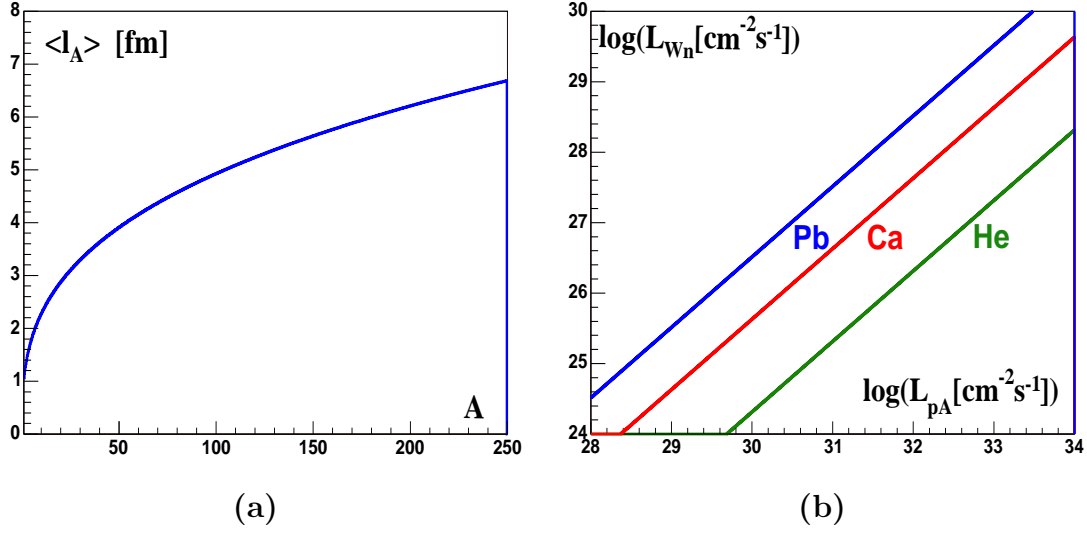


Figure 7: The effective target length, (a), and the  $W$ -nucleon luminosity, (b).

In Fig. 7a we show the dependence of the average path-length upon the atomic number of the target nucleus for the  $W$ -bosons satisfying the condition (25). The projected density was calculated using the Saxon-Woods density [31], and the nuclear radius was taken to be the Saxon-Woods parametrization radius. The dynamic range of the average path-length is confined to the distances of  $\sim 1$ –7 fm, depending on the atomic number of the target nucleus.

In order to demonstrate the full equivalence of the targets used in macroscopic scattering experiments with the nuclear targets for the femto-experiments, it remains to be demonstrated that the experimental control of the average length of the the  $W$ -boson beam target is equivalent to the event-by-event control of the target-length in macroscopic experiments. This need not to be the case in general. For the  $W$ -boson beam this requirement is likely to be fulfilled since the  $W$ -nucleon collision cross section is expected to be small enough that each produced  $W$ -boson could collide at most once within the nucleus:  $\sigma_{Wn} \ll 1 \text{ fm}^2$ . If this condition is fulfilled, then the sample of  $N$  events in which the  $W$ -boson traveled the total distance  $l_A(N) = \sum_{i=1,N} l_A(i)$  is, in the limit of large  $N$ , equivalent to the sample of  $N$  events in which each produced  $W$ -boson traveled the distance  $\langle l_A \rangle$  given by eq. (26).

---

where  $K(s_{Wn})$  varies between 1, for the lowest energies, and 2, for the highest energies of the  $W$ -nucleon collisions at the LHC.



## 6 Luminosity

The luminosity of the LHC  $W$ -nucleon collider, employing the polarized  $W$ -boson beam produced in the interaction of the primary beams of protons and ions of atomic number  $A$ , can be expressed as:

$$L_{Wn}^{\lambda_{in}}(s_{Wn}) [\text{fm}^{-2} \text{s}^{-1}] = \mathcal{F}_W^{\lambda_{in}}(s_{Wn}) [\text{s}^{-1}] \times \langle l_A(s_{Wn}) \rangle [\text{fm}] \times \rho_A^n [\text{fm}^{-3}]. \quad (27)$$

In this formula we have written explicitly the units and expressed the kinematic observables in terms of the Lorentz-invariant centre-of-mass energy of the  $W$ -nucleon collisions. The flux of the  $W$ -boson in the polarization state  $\lambda_{in}$  enters the equation in the surface-integrated form. This simplification was possible owing to the large  $\gamma$ -factor of the Lorentz-boost from the  $W$ -beam particle rest frame to the nuclear rest frame<sup>23</sup>, which reduces the apparent divergence of the  $W$ -beam in the target rest frame. The centre-of-mass energy of the  $W$ -nucleon collisions is unambiguously determined by the longitudinal momentum of the  $W$ -boson in the *collinear  $W$ -nucleon collision* frame because the Fermi momenta of the nucleons within the nuclei can be neglected at the LHC energies. Similar formula could also be written for the luminosity of  $W$ -parton collisions by replacing the distribution of the nucleons within the nucleus  $\rho_A^n$  with the distribution of the partons within the nucleus  $\rho_A^p$  and by recalculating the formula (22) for the partonic density rather than nucleon density. This would preclude that  $W$ -bosons interact with hadronic matter only by a direct coupling to its point like constituents. Such an assumption, even if quite natural, will have to be tested experimentally at the LHC.

In order to assess the statistical sensitivity of the  $W$ -nucleon collider for exploring the interactions of  $W$ -bosons with hadronic matter, we rewrite the formula (27) by expressing the  $W$ -boson flux in terms of the luminosity of the proton-nucleus collisions  $L_{pA}$ :

$$L_{Wn}^{\lambda_{in}}(s_{Wn}) = L_{pA} \sigma_{pA \rightarrow W+X}^{\lambda_{in}}(s_{Wn}) \langle l_A(s_{Wn}) \rangle \rho_A^n. \quad (28)$$

The dependence of the total  $W$ -nucleon collision luminosity, summed over all  $W$ -boson polarization states, upon the nucleon-nucleus collision luminosity is shown in Fig. 7b for three nuclear beams: helium, calcium and lead, and for the  $Wn$ -collision energies satisfying the condition of eq. (25). This plot illustrates what values of luminosities of the proton-helium, proton-calcium and proton-lead collisions need to be achieved for the required  $W$ -nucleon collision luminosity. If the luminosity of the  $p$ - $A$  collisions decreases with the atomic number of the nucleus as  $L_{pA} \sim L_{pp}/A$ , then the  $p$ - $Pb$  collisions are the most effective in reaching the highest possible sensitivity to the  $W$ -nucleon collision effects. If it will decrease faster, e.g. like  $L_{pA} \sim$

---

<sup>23</sup>The lower boundary of the Lorentz  $\gamma$ -factor depends upon the angular acceptance for the  $W$ -decay products of the LHC detector. In the case of the ATLAS (CMS) detector  $\gamma \geq 100$ .

$L_{pp}/(AZ)$ , then the beams of lighter nuclei may turn out to be more effective. Given the expected performance of the LHC collider for the proton–nucleus collisions, the sensitivity to the  $W$ –nucleon cross sections down to the level of 100 nb can be reached. The systematic sensitivity will be determined entirely by the quality of the dedicated analysis methods capable of reducing the overwhelming background to the  $W$ -boson collision effects due to conventional partonic processes.

One of the merits of the  $W$ -beam at the LHC collider is that it is a broad-momentum-band beam. It will give access to a broad range of the  $W$ –nucleon collision energies. The spectrum of energies of the  $W$ –nucleon collisions is shown in Fig. 8a. The accessible energies extend up to the TeV range – the region where collisions of the  $W$ -bosons, in particular the longitudinally polarized  $W$ -bosons, are expected to shed light on the mechanism of the electroweak symmetry breaking.

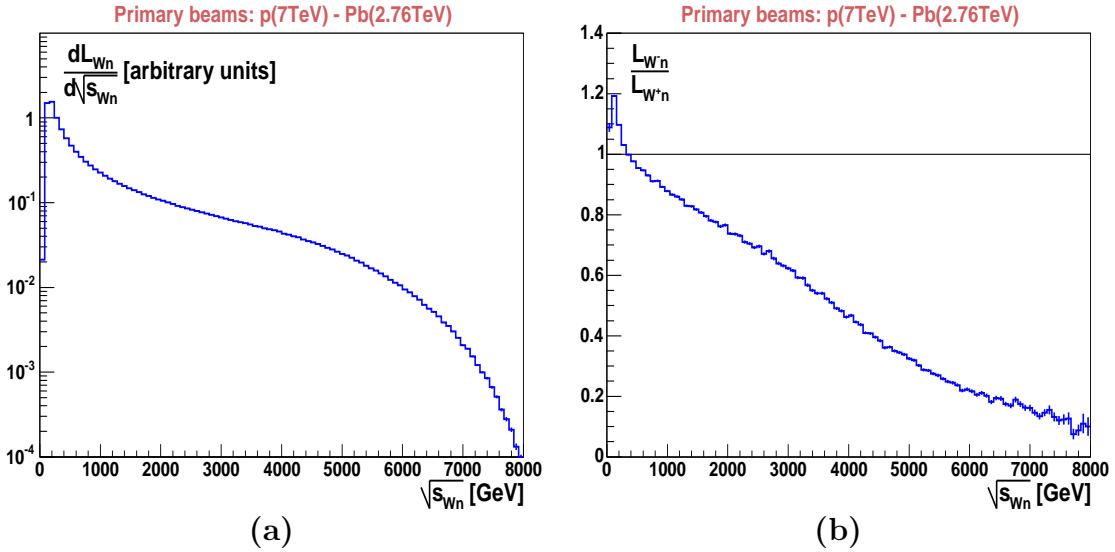


Figure 8: The distribution of the  $W$ –nucleon CMS energy, (a), and ratio of the collision-energy spectra for the  $W^+$  and  $W^-$  beams, (b).

In Fig. 8b we show the ratio of the energy spectra for positively and negatively charged  $W$ -bosons. This plot illustrates the merit of having simultaneous beams of positively and negatively charged  $W$ -bosons for exploring the energy dependence of the  $W$ –nucleon inclusive cross section. Even if the centre-of-mass energy of the  $W$ –nucleon collision is not directly reconstructed, the  $W^+$  and  $W^-$  spectra are sufficiently distinct to look for the anomalies in energy dependence of the cross section, in the abnormal effective-target-length dependence of the charge asymmetry of the final-state  $W$ -bosons.

## 7 Outlook

The luminosity the  $W$ -nucleon collisions that can be reached at the LHC may not be high enough to explore the rare  $W$ -boson collisions (e.g. the  $W$ - $W$  collisions). The sensitivity to such processes is inferior with respect to the canonical proton-proton (nucleon-nucleus) collisions, where the process of the virtual  $W$ -boson creation and its subsequent hard collision takes place in a single space-time volume<sup>24</sup>. The  $W$ -nucleon collisions will be optimal, for exploring “soft”  $W$ -boson collisions with hadronic matter, in particularly for investigating the processes sensitive to the polarization of the initial  $W$ -boson. Generic studies of such collisions may lead to surprises which are not present in the inventory lists of the canonical search scenarios.

The  $W$ -nucleon collision program at the LHC could start from the analysis of the electroweak-boson production in the proton-lead collisions. This configuration is already foreseen in the LHC collider program. Such studies could be considered as a “femto-detector R&D”, having as a goal to demonstrate the feasibility of extraction of the  $W$ -nucleon collision signals in the proton-lead collisions. If such a demonstration is made and the need for a generic exploration of the  $W$ -boson collisions at the LHC energies arise (either because of confirmation or because of rejection of the canonical scenarios of the electroweak symmetry breaking), the configuration phase of the femto-experiment could follow. Configuring the femto-experiment would consist of choosing the optimal nuclear species, beam energies and the running time in each of the LHC collider setting for the highest sensitivity to the  $W$ -nucleon collision effects.

## 8 Concluding Remarks

In this paper we have presented a generic, experimental method of exploring the processes of collisions of the  $W$ -bosons with hadronic matter in the TeV-energy range. We have shown that the collisions of the standard LHC beams can be treated as an incoherent source of the polarized, wide-momentum-band  $W$ -boson beam. Such a beam can be used to study the collisions of the  $W$ -bosons with nucleons in analogous way to the use of the muon beam in the fixed-target experiments. We have proposed a coherent data analysis framework allowing to relate both the spin-independent and the spin-dependent  $W$ -nucleon collision observables to the event rates measured in collisions of the primary LHC beams. We have discussed the unfolding method of the  $W$ -nucleon collision cross sections and proposed the experimental methods of controlling the spectra and the fluxes of the  $W$ -boson beam,

---

<sup>24</sup>The rare, hard  $W$ -nucleon collisions can be considered in this context as higher-twist processes in nucleon-nucleus collisions.

its polarization, and the effective lengths of the  $W$ -boson targets. The  $W$ -nucleon luminosities that can be achieved at the LHC reach the values of  $L = 10^{28} \text{ cm}^{-2} \text{ s}^{-1}$ .

In this paper we have not discussed the selection methods for filtering out the signals of the  $W$ -boson collisions from the background of ordinary nucleon-nucleus collisions. This subject will be addressed in [1].

The main purpose of this paper is to draw attention to a very important and unique merit of the LHC nuclear beams for the experimental program aiming to explore, in the model independent way, the collisions of electroweak bosons at the TeV energy scale. Such a program can be uniquely realized at the LHC collider owing to the versatility of its running modes and beam particle species. It can be realized neither at the lepton-beam colliders nor at the Tevatron collider. The luminous nuclear beams provide the indispensable research tools for such a program. While their merits for the QCD sector of the Standard Model, in particular for searches of the quark-gluon plasma, are widely accepted, their merits for studies of the electroweak sector of the Standard Model have, up to our best knowledge, not been put so far into sufficiently bright light. This paper could be considered as an attempt to fill in this gap by showing the unique role of the LHC collision scheme in which the light ions (protons) are colliding with the heavy ions.

## Acknowledgements

We would like to thank Y. Dokshitzer, F. Dydak and A. Białas for useful discussions.

## References

- [1] M. W. Krasny, S. Jadach, and W. Placzek, The Femto-experiment for the LHC:  $W$ -boson collisions with hadronic matter, in preparation.
- [2] B. L. Ioffe, Phys. Lett **B30**, 123 (1968).
- [3] ATLAS Collaboration, ATLAS Detector and Physics Performance Technical Design Report, CERN/LHCC/99-14, 25 May 1999.
- [4] D. Jackson, J., High Energy Physics (eds. C. de Wit and M. Jacob) **B35**, 327 (1965).
- [5] M. W. Krasny, Physics of  $eA$  collisions at RHIC, Introductory talk at the 2nd eRHIC workshop, Yale, April 6-8, 2000.
- [6] M. W. Krasny, Detector Issues of Lepton-Hadron Colliders, Presented at the Snowmass Workshop on the Future of High Energy Physics, Snowmass, July 6, 2001.

- [7] M. W. Krasny, Nucl. Phys. Proc. Suppl. **105**, 185 (2002).
- [8] R. Homberg, W. L. van Nerven, and T. Marsuura, Nucl. Phys. **B359**, 343 (1991).
- [9] Y. L. Dokshitzer, D. Diakonow, and S. I. Trojan, Phys. Lett. **B79**, 269 (1978).
- [10] U. Baur, S. Keller, and D. Wackerroth, Phys. Rev. **D59**, 013002 (1998).
- [11] S. Dittmaier and M. Kramer, Phys. Rev. , 073007 (2002).
- [12] W. Flaczek and S. Jadach, Eur. Phys. J. **C29**, 325 (2003), hep-ph/0302065.
- [13] S. Haywood *et al.*, *Electroweak Physics*, in [32].
- [14] P. M. Nadolsky, hep-ph0412146.
- [15] W. K. Tung, hep-ph0410139.
- [16] S. Jadach and M. Skrzypek, Acta Phys. Polon. **B35**, 745 (2004), hep-ph/0312355.
- [17] K. Golec-Biernat, S. Jadach, W. Flaczek, and M. Skrzypek, Markovian Monte Carlo solutions of the NLL QCD evolution equations, IFJPAN-V-04-08, in preparation.
- [18] S. Jadach and M. Skrzypek, Non-Markovian Monte Carlo Algorithm for the Constrained Markovian Evolution in QCD, IFJPAN-V-04-06, in preparation.
- [19] S. Jadach and M. Skrzypek, Solving Constrained Markovian Evolution in QCD with the help of Non-Markovian Monte Carlo, IFJPAN-V-04-07, in preparation.
- [20] W. Flaczek and S. Jadach, WINHAC 1.13: The Monte Carlo Event Generator for Single  $W$ -Boson Production with Leptonic Decays in Hadron Collisions, available from <http://cern.ch/placzek>.
- [21] H. Plathow-Besch, PDFLIB: Proton, pion and photon parton density functions, parton density functions of the nucleus, the  $\alpha_s$  calculations, H.Plathow-Besch/CERN-ETT/TT, 2000.04.17.
- [22] D. R. Yennie, S. Frautschi, and H. Suura, Ann. Phys. (NY) **13**, 379 (1961).
- [23] C. Carloni Calame, S. Jadach, G. Montagna, O. Nicrosini, and W. Flaczek, Acta. Phys. Polon. **B35**, 1643 (2004), hep-ph/0402235.
- [24] K. Escola, V. Kolhinen, and C. Salgado, Eur. Phys. J. **C9**, 61 (1999).

- [25] M. W. Krasny, A New Measurement of the Charged-Current Cross-Sections for the Neutrino and Antineutrino interactions, Proceedings of the International Conference on High Energy Physics, Bari, July 1985, eds. L. Nitti and G. Preparata, 1985.
- [26] J. P. Berge, Z. Phys. **C35**, 443 (1987), CERN-EP/87-09.
- [27] M. W. Krasny, Nucl. Instr. Meth. **A540**, 222 (2005).
- [28] M. W. Krasny, Nucl. Phys. **A622**, 95 (1997).
- [29] M. W. Krasny, Electron–nucleus collisions at HERA, Proceedings of the Joint DESI-GSI-NuPECC Workshop on Hadronic Physics in Europe, Seeheim, April, 1997, GSI REPORT 97–04, April 1997.
- [30] M. W. Krasny, Nucl. Phys. **A663**, 56 (2000), hep-ph/9907410.
- [31] D. Barrett, R. C. Jackson, Nuclear Sizes and Structure, Oxford University Press, 1977.
- [32] G. Altarelli and M. Mangano, editors, *Proceedings of the Workshop on Standard Model Physics (and More) at the LHC* (CERN 2000-004, Geneva, 2000).